
LeYOLO, New Scalable and Efficient CNN Architecture for Object Detection

Lilian Hollard*

Université de Reims Champagne-Ardenne
CEA, LRC DIGIT, LICIIS
Reims, France
lilian.hollard@univ-reims.fr

Lucas Mohimont

Université de Reims Champagne-Ardenne
CEA, LRC DIGIT, LICIIS
Reims, France
lucas.mohimont@univ-reims.fr

Nathalie Gaveau

Université de Reims Champagne-Ardenne
INRAE, RIBP USC 1488
Reims, France
nathalie.gaveau@univ-reims.fr

Luiz Angelo Steffanel

Université de Reims Champagne-Ardenne
CEA, LRC DIGIT, LICIIS
Reims, France
luiz-angelo.steffanel@univ-reims.fr

Abstract

Computational efficiency in deep neural networks is critical for object detection, especially as newer models prioritize speed over efficient computation (FLOP). This evolution has somewhat left behind embedded and mobile-oriented AI object detection applications. In this paper, we focus on design choices of neural network architectures for efficient object detection computation based on FLOP and propose several optimizations to enhance the efficiency of YOLO-based models.

Firstly, we introduce an efficient backbone scaling inspired by inverted bottlenecks and theoretical insights from the Information Bottleneck principle. Secondly, we present the Fast Pyramidal Architecture Network (FPAN), designed to facilitate fast multiscale feature sharing while reducing computational resources. Lastly, we propose a Decoupled Network-in-Network (DNiN) detection head engineered to deliver rapid yet lightweight computations for classification and regression tasks.

Building upon these optimizations and leveraging more efficient backbones, this paper contributes to a new scaling paradigm for object detection and YOLO-centric models called LeYOLO. Our contribution consistently outperforms existing models in various resource constraints, achieving unprecedented accuracy and flop ratio. Notably, LeYOLO-Small achieves a competitive mAP score of **38.2%** on the **COCO val** with just **4.5 FLOP(G)**, representing a **42% reduction** in computational load compared to the latest state-of-the-art YOLOv9-Tiny model while achieving similar accuracy. Our novel model family achieves a FLOP-to-accuracy ratio previously unattained, offering scalability that spans from ultra-low neural network configurations (< 1 GFLOP) to efficient yet demanding object detection setups (> 4 GFLOPs) with **25.2, 31.3, 35.2, 38.2, 39.3 and 41 mAP for 0.66, 1.47, 2.53, 4.51, 5.8 and 8.4 FLOP(G)**.

1 Introduction

In object detection, deep neural networks aim to extract a set of bounding boxes around each object of interest from a raw input image and categorize them into the correct class. Therefore, gathering rich spatial information is necessary to localize precisely different objects of interest.

*<https://github.com/LilianHollard/LeYOLO>

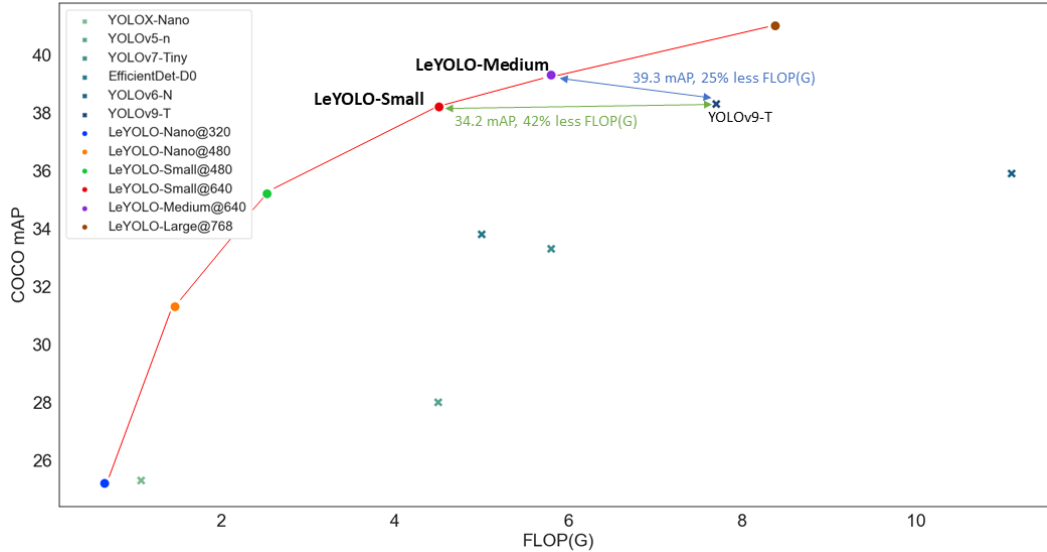


Figure 1: LeYOLO (ours) with other state-of-the-art efficient object detectors [25, 24, 14, 61, 12, 30, 64, 71, 2].

While deep neural networks have enabled impressive advancements, they heavily hinge on computationally expensive resources, limiting deployment on less powerful devices. Cloud offers an alternative to offload the execution of powerful models but it presents inconveniences like latency, bandwidth limitations, and security concerns [3, 80, 74]. Indeed, efficient computation, real-time processing, and low computational latency are crucial in practical applications such as autonomous driving, surveillance systems, medical imaging, and intelligent agriculture. Lightweight yet robust object detectors find their utilities in resource-constrained environments such as mobile and edge computing devices.

1.1 State-of-the-art

Deep neural networks have always been in close competition for solving classification, regression, segmentation, and object detection problems. Many state-of-the-art classification models [25, 54, 24, 41, 77, 43, 69, 10, 7, 10, 61, 18, 65] designed for mobile use serve as low-cost object detectors using the SSDLite neural network [38]. On the other hand, YOLO-type models optimized for execution speed [50–52, 2, 30, 32, 71, 73, 9, 78, 29], follows the evolution of computing resources, forsaking embedded devices. Fortunately, novel YOLO-based architectures embrace efficient computation, focusing on MAC and FLOP [45, 12, 14, 76, 16, 75]. These architectures present compelling evidence of their utility for edge AI and industrial applications, enhancing embedded devices and enabling direct model responses.

Indeed, there is a strong interest in "YOLO" models, which are equally popular in industry and non-computing research fields. Indeed, YOLO is used in medicine [1, 46, 67, 60], viticulture [56, 34, 55, 48, 22], and other fields [47, 33, 49]. Also, the ease of use and the fast execution make YOLO an excellent choice for researchers.

The panel of object detector possibilities extends to several options: object detection designed for speed [52, 2, 32, 9, 78, 71, 14, 51, 50, 73, 8, 30, 29], precision [53, 39, 6, 19], and the best ratio of precision (mAP) to calculation cost (FLOP)[12, 45, 38, 16, 14, 76, 75, 40] reducing the computational cost (FLOP) as much as possible. This last point should make us consider separating "low-cost" and "fast" models as if they did not correlate.

Recently, we saw an interesting pattern in the focus of YOLO models, with increasing emphasis on execution speed at the expense of computational cost [71, 73, 9, 78]. One major drawback of this computational cost is the necessity to consider memory access and the possibility of parallelizing convolution operations. With the apparent evolution of GPUs or, more generally, of computing resources, most authors have come to the unmistakable conclusion that it is now possible to add more

filters and parameters while formulating their architectures to parallelize the operations of a neural network as closely as possible. The phenomena increases model calculation costs (MAC or FLOP) while maintaining or improving model execution speed mostly thanks to GPU upgrades over the year.

The newest YOLO models [73, 8, 71], displayed as state-of-the-art in "lightweight" models under the guise of impressive execution speed and optimization on high-performance computing resources, still need to be improved for edge mobile devices.

We define a lightweight model as a neural network with few FLOP, no matter the number of parameters or execution speed. Some papers might use parameters to prove their model's "lightweight" capacity. However, the same number of parameters from a filter might have very different computing needs depending on the input spatial size, invalidating this solution. As for speed, while this metric is interesting, it is also biased regarding the computing resources. Therefore, we focus on FLOP to build an efficient object detector like EfficientDet [64], and we also provide parameters and speed to give readers a wide spectrum of comparisons (Chapter B.1).

We present **LeYOLO**, a conceptually simple yet efficient architecture that embraces computationally efficient components for object detection, following the cores of EfficientNets [62, 63], MobileNets [54, 25, 24], and similar innovations [35, 38, 77, 72, 28, 36, 20, 26, 41, 79, 23]. We aim to introduce a fresh architectural approach for YOLO models, prioritizing efficient scaling. This initiative seeks to empower mobile and embedded devices with enhanced capabilities.

We compare LeYOLO with other state-of-the-art efficient object detectors such as YOLOs, Efficient-Det and others [25, 24, 14, 61, 12, 30, 64, 71, 2]. Our evaluation focuses on MSCOCO [37] validation mAP and FLOP ratio, highlighting the importance of minimal computations for embedded devices. LeYOLO demonstrates superior performance across a broad scope of neural networks, surpassing ultra-low networks (less than 1 FLOP(G)), mid-range networks (between 1 and 4 FLOP(G)), and even models exceeding 4 FLOP(G), as illustrated in the Figure 1.

In all its versions, LeYOLO achieves 25.2%, 29%, 31.3%, 35.2%, 36.4%, 38.2%, 39.3% and 41% mAP on the MSCOCO validation dataset for 0.66, 1.126, 1.47, 2.53, 3.27, 4.51, 5.8 and 8.4 FLOP(G) as Table 3 shows.

Our main contributions are as follows:

1. **Lightweight:** Regarding the accuracy per FLOP ratio, LeYOLO achieves the best accuracy compared to state-of-the-art neural networks for lightweight object detection (between 0.5 to 8 FLOP(G)).
2. **Scaling:** LeYOLO offers a new opportunity to use lightweight YOLO models with state-of-the-art scaling efficiency for industry, edge, and embedded devices.
3. **Bags of specials:** Although our research focuses on the best ratio of precision to calculation cost, we propose different alternatives by referencing all the options we have discovered.
4. **New architecture:** We suggest new computationally efficient blocks for use in LeYOLO and provide proof through experimentation.
5. **High reproducibility:** Our research priority is improving the architecture of deep neural networks. We achieve the results using reusable training methods from the **ultralitics API**, without ImageNet [31] pre-training.

2 Description of the LeYOLO Architecture

2.1 Block definition

2.1.1 Base building block

The inverted bottleneck, initially invented by MobileNetV2 [25, 54], is the essence of many new state-of-the-art models [62, 63, 18, 65, 43, 38, 69] for its lightweight computation and simplicity. It is complex to achieve a level of effectiveness surpassing depthwise convolutions in terms of FLOP computation. Pointwise convolutions address the absence of channel-wise correlations, which are difficult to work without. Nevertheless, in our experiments with the inverted bottleneck block, we observed that optimizing the number of channels could reduce efficiently the computation needs, especially at large spatial feature map sizes. Indeed, if a block's expansion ratio is equal to one or if,

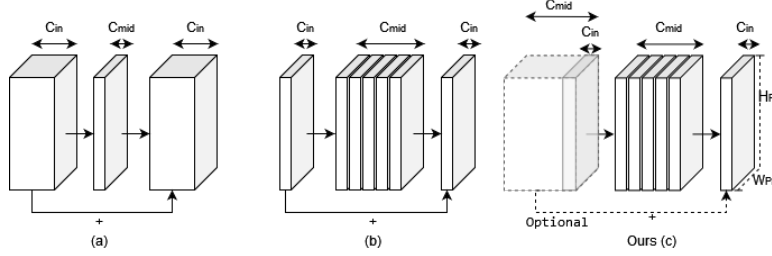


Figure 2: Base building block of LeYOLO (c), highlighting the distinctions between the classical bottleneck (a), inverted bottleneck (b) [25, 54, 24], and our proposed approach (c).

by concatenation effect, the incoming channels C_{in} are equal to the calculated number of extended layers C_{mid} , there is no need to use the first pointwise convolution in our block. We always use the residual connection even if the first pointwise does not exist, as long as the incoming C_{in} and outgoing C_{out} tensor are equal as Figure 2 and Equation (1) shows. We depict the base building block of LeYOLO in Figure 2(c), highlighting the distinctions between the classical bottleneck (Figure 2(a)), inverted bottleneck (Figure 2(b)) [25, 54, 24], and our proposed approach (Figure 2(c)).

We denote \otimes as a convolution between two values. For $F_{in} \in \mathbb{R}^{1,1,C_{in},C_{mid}}$, $F_{out} \in \mathbb{R}^{1,1,C_{mid},C_{out}}$ and $F_{mid} \in \mathbb{R}^{k,k,1,C_{mid}}$ the convolutions with C_{in} as the number of input channel, C_{mid} the number of expanded channel in the inverted bottleneck and C_{out} the number of output channel :

$$y = \begin{cases} F_{out} \otimes [F_{mid} \otimes (F_{in} \otimes x)] & \text{if } C_{in} \neq C_{mid} \\ F_{out} \otimes [F_{mid} \otimes (F_{in} \otimes x)] & \text{if } C_{in} = C_{mid} \text{ and } F_{in} = \text{True} \\ F_{out} \otimes [F_{mid} \otimes (x)] & \text{if } C_{in} = C_{mid} \text{ and } F_{in} = \text{False} \end{cases} \quad (1)$$

Similar to the state-of-the-art neural network techniques for object detection [71, 73], we consistently implement the SiLU [11] activation function throughout our model.

2.1.2 Stride strategy

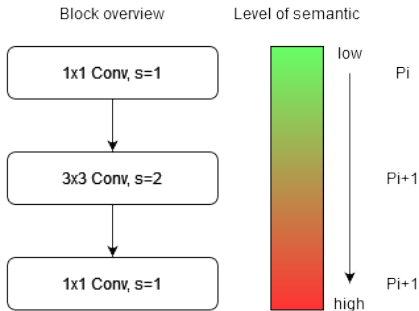


Figure 3: Inverse Bottleneck semantic information variations.

Several models incorporate stride within the inverted bottleneck [25, 54, 24, 75, 63, 43, 70, 44]. However, we employ a **specific channel expansion strategy**.

Every semantic level of information denoted as P_i consistently has its number of input $C_{in}P_i$, output $C_{out}P_i$, and expanded channels $C_{mid}P_i$ throughout all its hidden layers. We aim to enrich the information flow from hidden layer h_i at the semantic information level P_i to the subsequent hidden layer h_{i+1} by increasing the channels $C_{in}P_i$ proportionately to the anticipated channel expansion from $C_{mid}P_{i+1}$.

With the inverted bottleneck taking the following steps:

$$h_i = F_{out} \otimes [F_{mid} \otimes (F_{in} \otimes x)] \quad (2)$$

The semantic information inside an strided inverted bottleneck denoted as P is as follows - Figure 3:

$$P_i \rightarrow P_{i+1} \rightarrow P_{i+1} \quad (3)$$

Therefore, the channel expansion strategy with a stride greater than one may resemble the following form:

$$C_{in}P_i \rightarrow C_{mid}P_{i+1} \rightarrow C_{out}P_{i+1} \quad \text{with } C_{mid}P_{i+1} > C_{mid}P_i \quad (4)$$

We could simply apply a rich expansion ratio to each block, not just those with a stride greater than one, but doing so would **significantly** increase the overall network cost.

While this strategy is not mandatory for the entire model, it does make sense at certain junctures, such as the stem, to maximize information expansion from expensive feature map spatial sizes, particularly with an ultimate pointwise convolution.

2.2 STEM

We often refer to the term "STEM" to describe the first layers, dealing directly with the input image and low semantic information to quickly and efficiently reduce the spatial size and excite the initial information channel count (regularly 3 for red, green, and blue) to a higher channel count. The main benefit is reducing the computational cost since the total cost quickly explodes for object detection if the layers processed are too large spatially. Only YOLOv7 [71] use no strided convolution from the first layer. The initial P0 (640x640 - 1280x1280) spatial size is too costly.

Looking at a sample of state-of-the-art YOLOs, only YOLOv6 [32], and YOLOv8 [29] are good examples of stems with low computational resources with a total cost of 0.32 GFLOP for both of them when scaling down the number of channels and layers to x0.25. These two models quickly scale down to 160x160p feature map to compensate for the cost of sliding convolutions on spatial sizes that are too high.

To efficiently use convolutions at large feature map sizes, we use **pointwise** with **standard** convolutions, limited to a strict low channel number throughout the whole STEM, to go from P0 (640x640) to P2 (160x160) - Table 1.

Table 1: Stem architecture overview for LeYOLO-small.

Block	Out channels	Kernel size	Stride	Activation	Output dimension
Conv+bn+act	16	3	2	SiLU	320x320
Conv+bn+act	16	1	1	SiLU	320x320
Depthwise+bn+act	16	3	2	SiLU	160x160
Conv+bn	16	1	1	SiLU	160x160
Total cost					0.3244 GFlop

2.3 Efficient backbone feature extractor

Historically, object detectors have been extensively supplemented for classification [53, 19, 38], leading to observing models using classical classification models as feature extractors.

Firstly, we use an inverted bottleneck for its unrivaled computational cost and cost-accuracy ratio.

Finally, for the choice of the number of layers, we made an obvious observation based on the state of the art of neural networks: there is a **focus** on layer repetition on **P4 or equivalent**.

Even more interestingly, using a NAS-type algorithm to select the number of layers or repetitions, we observe the same phenomenon: layers at P4 receive more importance than others [25, 62, 63, 61, 15, 4]. We made this observation based on a selection of YOLO [52, 2, 30, 32], as shown in Table 2.3 but also on classification models using convolutions [77, 41, 58, 57, 59], self-attention [42–44, 68, 39], and finally, object detectors like DETR [6] based on ResNet [20], which also focuses on equivalent P4 middle-flow.

We cannot afford to rely so heavily on P3 like [52, 2, 32] to create a neural network based on low computational cost. Therefore, our backbone uses the number of repetitions shown in Table 2.3 (strided inverted bottleneck included).

2.3.1 Information Bottleneck Characteristic's

The information bottleneck principle theory from [66] highlight two critical aspects of learning theory concerning information. Firstly, the authors recognize that deep neural networks (DNNs) **deviate** from being precisely Markov Chains [13] as $X \rightarrow \tilde{X} \rightarrow Y$ with X , \tilde{X} and Y being the input, the minimal sufficient statistics extracted from X and the output respectively.

Table 2: Layer repetition in state-of-the-art compared to our contribution.

Models	P3	P4	P5
YOLOv3 [52]	x8	x8	x4
YOLOv4 [2]	x8	x8	x4
YOLOv5 [30]	x6	x9	x3
YOLOv6 [32]	x12	x12	x6
LeYOLO-Nano	x2	x5	x4

Consequently, to derive \tilde{X} as the minimal sufficient statistics for extracting meaningful features to address Y , DNNs need to learn how to extract features using minimal sufficient statistics, employing the **most compact architecture** possible [66].

Secondly, because DNNs only process inputs from the preceding layer h_{i-1} , a direct implication involves potentially losing information that subsequent layers cannot regain (equation (5)).

$$I(Y; X) \geq I(Y; h_i) \geq I(Y; h_{i+j}) \quad \text{with} \quad i + j \geq i \quad (5)$$

Expensive solutions such as column-oriented networks [5, 21] with intensive feature sharing between each block address this issue by incorporating intensive training blocks or adding additional detection heads at crucial points of information segmentation, as seen very recently in YOLOv9 [73]. As achieving equity in the equation above is feasible, the theory [66] suggests that each layer should maximize information within itself $I(Y; h_i)$ while minimizing inter-layer information exchange as much as possible $I(h_{i-1}; h_i)$. Hence, rather than augmenting computational complexity in our model like [71, 73, 21, 5], we opted to scale it more efficiently, integrating Dangyoon’s at al. [17] inverted bottleneck theory.

Our implementation involves minimizing inter-layer information exchange in the form of $I(h_0; h_n)$, with n equal to the last hidden layer of the neural network, by ensuring that the number of input/output channels never exceeds a difference ratio of the first hidden layer through to the last. The number of hidden layer channels should stay within a limit defined by the input channels at P1 and the output channel at P5, with a difference ratio of less than 6, minimizing $I(h_{i-1}; h_i)$ in the form of $I(h_1; h_n)$.

$$C_{h_i} \in [C_{h_1}; C_{h_n}] \quad \text{with} \quad \frac{C_{h_n}}{C_{h_1}} \leq 6 \quad (6)$$

Conversely, the inverted bottleneck channel expansion experimentations from Dangyonn et al. [17] show that an expansion or reduction ratio should never exceed 6. Therefore, we maximize $I(Y; h_i)$ with an expansion of 3 in the whole network. Also, during a stridded inverted bottleneck with a pointwise channels expansion strategy, the information is excited further with a total expansion of 6, maximizing $I(Y; h_i)$ in between $(P_i; P_{i+1})$. However, we excite the information further from the inverted bottleneck of $P4$ to $P5$, maximizing $I(Y; h_i)$ at $(P4; P5)$ with an expansion of 9 (+0.5 mAP compared to an expansion of 6, more information in Chapter B.3 and B.4).

The implementation of residual connections between blocks helps minimize $I(h_{i-1}; h_i)$ by providing information from the preceding layer h_{i-1} . Dense connections [16, 27] may enhance the model, but, they require additional memory.

2.4 Neck

In object detection, we call neck, the part of the model that aggregates several levels of semantic information, sharing extraction levels from more distant layers to the first layers.

Historically, researchers have used a PANet [79] or FPN [36] to share feature maps efficiently, enabling multiple detection levels by linking several semantic information P_i to the PANet and their respective outputs as depicted in Figure 4(a).

In this paper, we are mainly focusing on two competitors: BiFPN [64] and YOLOF’s SiSO [8]. BiFPN shares our model’s central philosophy: using layers with low computational cost (concatenation and additions, depthwise and pointwise convolutions). However, BiFPN requires too much semantic

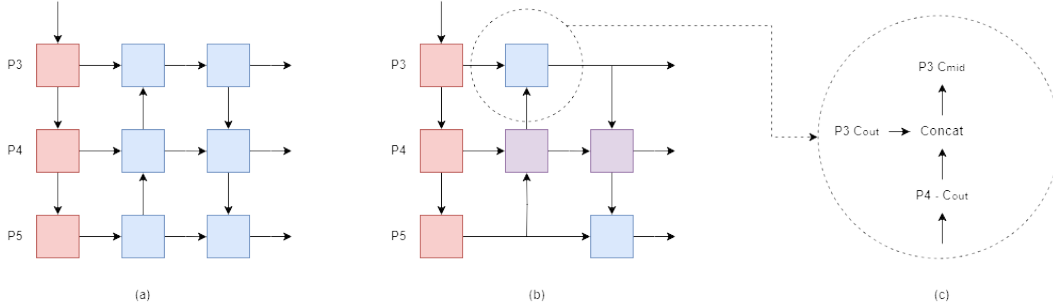


Figure 4: Computational distinction between classic PANet [79] and FPANet (our model).

information and too many blocking states (waiting for previous layers, complex graphs), which makes it difficult to keep up with fast execution speed.

SiSO [8], on the other hand, is interesting in its approach to object detection. Indeed, we can see that the authors of YOLOF have decided to use a single input and output for the model neck. Compared with other proposed solutions in YOLOF paper, we observe a significant degradation between a neck with multiple outputs (Single-in, Multiple-out - SiMO) and a neck with a single output (Single-in, Single-out - SiSO). We are particularly interested in their work on the potential efficiency of a SiMO, proving the possibility of improving the first layers of the neck of a YOLO model by optimizing the flow of semantic information with only one rich input.

Drawing inspiration from PAN and FPNnet, we propose a Fast PANnet (FPANet) featuring fewer convolution layers, low number of channels and more efficient sharing of semantic information. Our approach shares similarities with the neck concept in YOLOv8 [29]. We reduced the computational flow between $P3$ and $P5$ post-backbone and right before the head, strengthening semantic information levels directly into $P4$, as depicted in Figure 4(b). Additionally, we simplified the neck, minimizing locks and waiting time, given the limited parallelization opportunities and complexities of the architecture. Moreover, as demonstrated in the Figure 4(c), we optimized channel numbers to reduce computation in $P3$, where the initial pointwise step is unnecessary, as the concatenation of the bottom-up pathway from $P4$ and $P3$ information from the backbone matches the expanded channels in the inverted bottleneck of PAN at $P3$, as $C_{out}P4 + C_{in}P3 = C_{mid}P3$.

By strengthening a single input ($P4$) with minimal computations from $P3$ and $P5$ to guide neck information, we have implemented an in-between of SiMO and MiMO approach with a significantly reduced variation of MiMO.

2.5 Decoupled Network in Network Head

Until YOLOv5 [50–52, 2, 30], we had single model heads for classification and object detection. However, since YOLOv6 [32], the model head has become a more powerful tool, separating the block into two parts: a branch for classification and object regression. Although very efficient, this implies an almost doubled cost, requiring convolutions for classification and detection.

We theorize that there is no need to add spatial information other than to refine the features extracted by the backbone and neck channels-by-channels using lightweight depthwise convolutions.

Historically, YOLO models work as a grid, proposing a classification for each grid pixel affined by anchor boxes at each point. Anchor boxes offered several possible detection sizes, not only pixel-wise detection.

Through YOLO’s point-by-point grid operation, we theorize that it is possible to simplify detection heads using pointwise convolution as a sliding multi-layer perceptron solution pixel by pixel, resembling classification propositions for each pixel—several depthwise convolutions for spatial-only instructions, refines spatial relationship in between two pointwise classifying and regressing each pixel.

With an ablation study (see Chapter B.4), we prove that using only pointwise convolutions at the head of the model yields impressive results with 33.4 mAP at the LeYOLO-Nano@640 scale. Refining

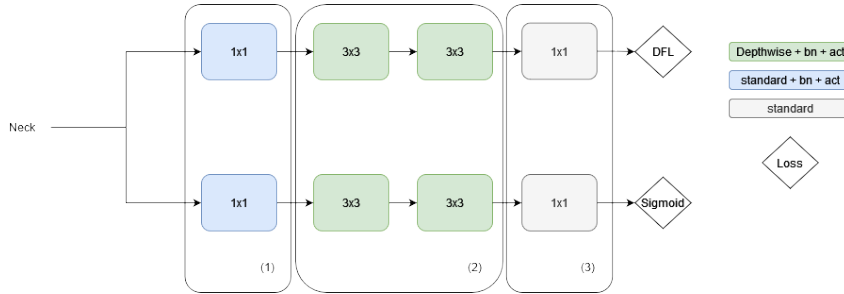


Figure 5: In the detection head of LeYOLO, we propose DNIN (Decoupled Network-in-Network) Head.

spatial information with depthwise convolution between pointwise convolutions pushes the model to **34.3 mAP**.

As figure 5 shows, we propose DNIN (Decoupled Network-in-Network Head), a pointwise-centered approach with two separate pointwise operations for each network proposal: classification and regression (bounding boxes). Pointwise operations are essential in object detection, serving as pixel-by-pixel classifiers and regressors within a network-in-network framework. Depthwise convolutions are split into two 3x3 convolutions to lower the overall cost compared to a single 5x5 convolution.

We operate two separate pointwise convolutions: one dedicated to classification and the other to regression. The distinction emerges from differing requirements between classification and bounding box extraction. Our proposed DNIN head expands channels to match class numbers while maintaining spatial dimensions at level P_i . Each pixel thus represents a potential prediction. Employing 1x1 convolutions refers to neural network origins, notably the NiN model [35], wherein pointwise convolutions emerged as a substitute for the conventional multi-layer perceptron.

2.6 Results

2.6.1 Architecture scaling

For LeYOLO, we offer a variety of models inspired by the architectural base presented above. A classic approach involves scaling the number of channels, layers, and input image size. Traditionally, scaling emphasizes channel and layer configurations, sometimes incorporating various scaling patterns. As the LeYOLO model’s stem, neck, and head are optimized, increasing the image size above 640 does not involve a drastically high FLOP. We offer eight versions of LeYOLO, with scaling discussed in Chapters B.4.4, from 320 to 768p, from 0.66 to 8.4 FLOP(G) as presented in Table 3.

3 Discussions

As we try to offer thorough theoretical insights from state-of-the-art neural networks to craft optimized solutions, we acknowledge several areas for potential improvement, and we cannot wait to see further research advancements with **LeYOLO**.

Channels selection: Our research still has uncertainties despite grounding our network design in the optimal information principle theory. Observing papers on Neural Architecture Search (NAS) reveals that the potential choices for channel configurations are vast and often beyond human intuition. Without NAS, it is challenging to affirm the selection of a specific number of channels with robust theoretical evidence. We anticipate that NAS could facilitate the discovery of better layer repetitions and channel configurations.

LeYOLO FPANet + DNIN Head: Considering the cost-effectiveness of our FPANet and model head, there is a significant opportunity for experimentation across different backbones of state-of-the-art classification models. LeYOLO emerges as a promising alternative to SSD and SSDLite. The promising results achieved on MSCOCO with our solution suggest potential applicability to other classification-oriented models. We focused our optimization efforts specifically on **MSCOCO**

Table 3: State-of-the-art lightweight object detector.

Models	Input Size	mAP	mAP50	mAP75	S	M	L	FLOP(G)
MobileNetv3-S[25]	320	16.1	-	-	-	-	-	0.32
MobileNetv2-x0.5[54]	320	16.6	-	-	-	-	-	0.54
MnasNet-x0.5[61]	320	18.5	-	-	-	-	-	0.58
LeYOLO-Nano	320	25.2	37.7	26.4	5.5	23.7	48.0	0.66
MobileNetv3[24]	320	22	-	-	-	-	-	1.02
YOLOX-Nano[14]	320	25.3	-	-	-	-	-	1.08
NanoDet	-	23.5	-	-	-	-	-	1.2
LeYOLO-Small	320	29	42.9	30.6	6.5	29.1	53.4	1.126
LeYOLO-Nano	480	31.3	46.0	33.2	10.5	33.1	52.7	1.47
MobileNetv2[54]	320	22.1	-	-	-	-	-	1.6
MnasNet[61]	320	23	-	-	-	-	-	1.68
LeYOLO-Small	480	35.2	50.5	37.5	13.3	38.1	55.7	2.53
Tinier-YOLO	-	17	34	15.7	4.8	17.3	26.8	2.563
MobileNetv1[25]	320	22.2	-	-	-	-	-	2.6
LeYOLO-Medium	480	36.4	52.0	38.9	14.3	40.1	58.1	3.27
LeYOLO-Small	640	38.2	54.1	41.3	17.6	42.2	55.1	4.5
YOLOv5-n[30]	640	28	45.7	-	-	-	-	4.5
EfficientDet-D0[64]	512	33.80	52.2	35.8	12	38.3	51.2	5
LeYOLO-Medium	640	39.3	55.7	42.5	18.8	44.1	56.1	5.8
YOLOv7-Tiny[71]	416	33.3	49.9	-	-	-	-	5.8
YOLOX-Tiny[14]	416	32.8	50.3	-	-	-	-	6.5
YOLOv4-tiny[2]	-	21.7	-	-	-	-	-	6.96
YOLOv9-Tiny[73]	640	38.3	53.1	41.3	-	-	-	7.7
LeYOLO-Large	768	41	57.9	44.3	21.9	46.1	56.8	8.4
YOLOv6-N[32]	640	35.9	51.2	-	-	-	-	11.1

and YOLO-oriented networks. However, we encourage experimentation with our solution on other datasets as well.

Computational efficiency: We have implemented a new scaling for YOLO models, proving that it is possible to achieve very high levels of accuracy while using very few computational resources (FLOP). Nevertheless, we are not the fastest in the state of the art, as there are speed imperfections due to the (deliberate) lack of parallelizable architecture like our predecessors [54, 24, 64]. We could further analyze scaling for different edge powers to propose parallelizable column and block scaling.

Hence, we encourage further experimentation with our proposal, going deeper into experimental outcomes while exploring various dataset variants tailored to specific industry needs, such as intelligent agriculture and medicine.

4 Conclusion

This paper presents advancements in lightweight object detection suitable for mobile applications, introducing a novel scaling approach for YOLO models. Our proposed architecture, FPAN and DNiN, use lightweight operations like pointwise and depthwise convolutions, offering a highly efficient neural network explicitly crafted for object detection, as lightweight as SDDLite based solutions. This breaks new ground in the cost-to-accuracy ratio. Building these optimizations leverages more efficient YOLO scaling. We propose a new family of YOLO models achieving competitive mAP scores on MSCOCO, focusing on a spectrum of FLOP resource constraints. Our scaled LeYOLO-Small achieves similar accuracy with 42% less FLOP than the newest state-of-the-art object detectors. In this way, we demonstrate that scaling and optimized channel selection between the different levels of semantic information can enable us to exceed the unprecedented FLOP per mAP ratio. LeYOLO-Medium outperforms the latest YOLOv9-Tiny state-of-the-art with 39.3 mAP (+2.61%) and 5.8 FLOP(G) (-24.67%).

Acknowledgments and Disclosure of Funding

This work was supported by Chips Joint Undertaking (Chips JU) in EdgeAI “Edge AI Technologies for Optimised Performance Embedded Processing” project, grant agreement No 101097300.

References

- [1] Mohammed A. Al-masni, Mugahed A. Al-antari, Jeong-Min Park, Geon Gi, Tae-Yeon Kim, Patricio Rivera, Edwin Valarezo, Mun-Taek Choi, Seung-Moo Han, and Tae-Seong Kim. Simultaneous detection and classification of breast masses in digital mammograms via a deep learning YOLO-based CAD system. *Computer Methods and Programs in Biomedicine*, 157:85–94, April 2018.
- [2] Alexey Bochkovskiy, Chien-Yao Wang, and Hong-Yuan Mark Liao. Yolov4: Optimal speed and accuracy of object detection. *arXiv preprint arXiv:2004.10934*, April 2020.
- [3] Rajkumar Buyya, Chee Shin Yeo, Srikumar Venugopal, James Broberg, and Ivona Brandic. Cloud computing and emerging IT platforms: Vision, hype, and reality for delivering computing as the 5th utility. *Future Generation Computer Systems*, 25(6):599–616, June 2009.
- [4] Han Cai, Ligeng Zhu, and Song Han. Proxylessnas: Direct neural architecture search on target task and hardware. *International Conference on Learning Representations*, arXiv:1812.00332, 2018.
- [5] Yuxuan Cai, Yizhuang Zhou, Qi Han, Jianjian Sun, Xiangwen Kong, Jun Li, and Xiangyu Zhang. Reversible column networks. *arXiv preprint arXiv:2212.11696*, 2023.
- [6] Nicolas Carion, Francisco Massa, Gabriel Synnaeve, Nicolas Usunier, Alexander Kirillov, and Sergey Zagoruyko. End-to-End Object Detection with Transformers. In Andrea Vedaldi, Horst Bischof, Thomas Brox, and Jan-Michael Frahm, editors, *Computer Vision – ECCV 2020*, pages 213–229, Cham, 2020.
- [7] Chengpeng Chen, Zichao Guo, Haien Zeng, Pengfei Xiong, and Jian Dong. Repghost: a hardware-efficient ghost module via re-parameterization. *arXiv preprint arXiv:2211.06088*, 2022.
- [8] Qiang Chen, Yingming Wang, Tong Yang, Xiangyu Zhang, Jian Cheng, and Jian Sun. You only look one-level feature. In *Proceedings of the IEEE/CVF conference on computer vision and pattern recognition*, pages 13039–13048, 2021.
- [9] Yuming Chen, Xinbin Yuan, Ruiqi Wu, Jiabao Wang, Qibin Hou, and Ming-Ming Cheng. Yolo-ms: rethinking multi-scale representation learning for real-time object detection. *arXiv preprint arXiv:2308.05480*, 2023.
- [10] Xiaohan Ding, Xiangyu Zhang, Ningning Ma, Jungong Han, Guiguang Ding, and Jian Sun. Repvgg: Making vgg-style convnets great again. In *Proceedings of the IEEE/CVF conference on computer vision and pattern recognition*, pages 13733–13742, 2021.
- [11] Stefan Elfving, Eiji Uchibe, and Kenji Doya. Sigmoid-weighted linear units for neural network function approximation in reinforcement learning. *Neural Networks*, 107:3–11, November 2018.
- [12] Wei Fang, Lin Wang, and Peiming Ren. Tinier-YOLO: A Real-Time Object Detection Method for Constrained Environments. *IEEE Access*, 8:1935–1944, 2020.
- [13] Paul A. Gagniac. *Markov Chains: From Theory To Implementation And Experimentation*. John Wiley and Sons, Inc, 2017.
- [14] Zheng Ge, Songtao Liu, Feng Wang, Zeming Li, and Jian Sun. Yolox: Exceeding yolo series in 2021. *arXiv preprint arXiv:2107.08430*, August 2021.
- [15] Golnaz Ghiasi, Tsung-Yi Lin, and Quoc V Le. Nas-fpn: Learning scalable feature pyramid architecture for object detection. In *Proceedings of the IEEE/CVF conference on computer vision and pattern recognition*, pages 7036–7045, 2019.

- [16] Mohammad Hajizadeh, Mohammad Sabokrou, and Adel Rahmani. MobileDenseNet: A new approach to object detection on mobile devices. *Expert Systems with Applications*, 215:119348, April 2023.
- [17] Dongyoon Han, Sangdoon Yun, Byeongho Heo, and YoungJoon Yoo. Rethinking channel dimensions for efficient model design. In *Proceedings of the IEEE/CVF conference on Computer Vision and Pattern Recognition*, pages 732–741, 2021.
- [18] Kai Han, Yunhe Wang, Qi Tian, Jianyuan Guo, Chunjing Xu, and Chang Xu. Ghostnet: More features from cheap operations. In *Proceedings of the IEEE/CVF conference on computer vision and pattern recognition*, pages 1580–1589, 2020.
- [19] Kaiming He, Georgia Gkioxari, Piotr Dollar, and Ross Girshick. Mask r-cnn. In *Proceedings of the IEEE International Conference on Computer Vision (ICCV)*, pages 2961–2969, Oct 2017.
- [20] Kaiming He, Xiangyu Zhang, Shaoqing Ren, and Jian Sun. Deep residual learning for image recognition. In *Proceedings of the IEEE conference on computer vision and pattern recognition*, pages 770–778, 2016.
- [21] Geoffrey Hinton. How to Represent Part-Whole Hierarchies in a Neural Network. *Neural Computation*, 35(3):413–452, February 2023.
- [22] Lilian Hollard and Lucas Mohimont. Applying Knowledge Distillation on Pre-Trained Model for Early Grapevine Detection. In *Workshop Proceedings of the 19th International Conference on Intelligent Environments (IE2023)*, pages 149–156. IOS Press, 2023.
- [23] Lilian Hollard, Lucas Mohimont, and Luiz Angelo Steffenel. Designing Lightweight CNN for Images: Architectural Components and Techniques. In *Advancing Edge Artificial Intelligence*. River Publishers, 2024.
- [24] Andrew Howard, Mark Sandler, Grace Chu, Liang-Chieh Chen, Bo Chen, Mingxing Tan, Weijun Wang, Yukun Zhu, Ruoming Pang, Vijay Vasudevan, et al. Searching for mobilenetv3. In *Proceedings of the IEEE/CVF international conference on computer vision*, pages 1314–1324, 2019.
- [25] Andrew G Howard, Menglong Zhu, Bo Chen, Dmitry Kalenichenko, Weijun Wang, Tobias Weyand, Marco Andreetto, and Hartwig Adam. Mobilenets: Efficient convolutional neural networks for mobile vision applications. *arXiv preprint arXiv:1704.04861*, 2017.
- [26] Jie Hu, Li Shen, and Gang Sun. Squeeze-and-excitation networks. In *Proceedings of the IEEE conference on computer vision and pattern recognition*, pages 7132–7141, 2018.
- [27] Gao Huang, Zhuang Liu, Laurens Van Der Maaten, and Kilian Q Weinberger. Densely connected convolutional networks. In *Proceedings of the IEEE conference on computer vision and pattern recognition*, pages 4700–4708, 2017.
- [28] Forrest N Iandola, Song Han, Matthew W Moskewicz, Khalid Ashraf, William J Dally, and Kurt Keutzer. Squeezenet: Alexnet-level accuracy with 50x fewer parameters and < 0.5 mb model size. *arXiv preprint arXiv:1602.07360*, 2016.
- [29] Glenn Jocher, Ayush Chaurasia, and Jing Qiu. Ultralytics YOLO, January 2023.
- [30] Glenn Jocher, Ayush Chaurasia, Alex Stoken, Jirka Borovec, NanoCode012, Yonghye Kwon, Kalen Michael, TaoXie, Jiacong Fang, imyhxy, Lorna, (Zeng Yifu), Colin Wong, Abhiram V, Diego Montes, Zhiqiang Wang, Cristi Fati, Jebastin Nadar, Laughing, UnglvKitDe, Victor Sonck, tkianai, yxNONG, Piotr Skalski, Adam Hogan, Dhruv Nair, Max Strobel, and Mrinal Jain. ultralytics/yolov5: v7.0 - YOLOv5 SOTA Realtime Instance Segmentation, November 2022.
- [31] Alex Krizhevsky, Ilya Sutskever, and Geoffrey E Hinton. ImageNet Classification with Deep Convolutional Neural Networks. In *Advances in Neural Information Processing Systems*, volume 25. Curran Associates, Inc., 2012.

- [32] Chuyi Li, Lulu Li, Hongliang Jiang, Kaiheng Weng, Yifei Geng, Liang Li, Zaidan Ke, Qingyuan Li, Meng Cheng, Weiqiang Nie, et al. Yolov6: A single-stage object detection framework for industrial applications. *arXiv preprint arXiv:2209.02976*, September 2022.
- [33] Gang Li, Shilong Zhao, Mingle Zhou, Min Li, Rui Shao, Zekai Zhang, and Delong Han. Yolorrff: An industrial defect detection method based on expanded field of feeling and feature fusion. *Electronics*, 11(24):4211, 2022.
- [34] Huipeng Li, Changyong Li, Guibin Li, and Lixin Chen. A real-time table grape detection method based on improved YOLOv4-tiny network in complex background. *Biosystems Engineering*, 212:347–359, December 2021.
- [35] Min Lin, Qiang Chen, and Shuicheng Yan. Network in network. *arXiv preprint arXiv:1312.4400*, 2013.
- [36] Tsung-Yi Lin, Piotr Dollár, Ross Girshick, Kaiming He, Bharath Hariharan, and Serge Belongie. Feature pyramid networks for object detection. In *Proceedings of the IEEE conference on computer vision and pattern recognition*, pages 2117–2125, 2017.
- [37] Tsung-Yi Lin, Michael Maire, Serge Belongie, James Hays, Pietro Perona, Deva Ramanan, Piotr Dollár, and C Lawrence Zitnick. Microsoft coco: Common objects in context. In *Computer Vision—ECCV 2014: 13th European Conference, Zurich, Switzerland, September 6–12, 2014, Proceedings, Part V 13*, pages 740–755. Springer, 2014.
- [38] Wei Liu, Dragomir Anguelov, Dumitru Erhan, Christian Szegedy, Scott Reed, Cheng-Yang Fu, and Alexander C. Berg. Ssd: Single shot multibox detector. In Bastian Leibe, Jiri Matas, Nicu Sebe, and Max Welling, editors, *Computer Vision – ECCV 2016*, pages 21–37, Cham, 2016.
- [39] Ze Liu, Yutong Lin, Yue Cao, Han Hu, Yixuan Wei, Zheng Zhang, Stephen Lin, and Baining Guo. Swin transformer: Hierarchical vision transformer using shifted windows. In *Proceedings of the IEEE/CVF international conference on computer vision*, pages 10012–10022, 2021.
- [40] Yonghui Lu, Langwen Zhang, and Wei Xie. YOLO-compact: An Efficient YOLO Network for Single Category Real-time Object Detection. In *2020 Chinese Control And Decision Conference (CCDC)*, pages 1931–1936, August 2020.
- [41] Ningning Ma, Xiangyu Zhang, Hai-Tao Zheng, and Jian Sun. Shufflenet v2: Practical guidelines for efficient cnn architecture design. In *Proceedings of the European conference on computer vision (ECCV)*, pages 116–131, 2018.
- [42] Muhammad Maaz, Abdelrahman Shaker, Hisham Cholakkal, Salman Khan, Syed Waqas Zamir, Rao Muhammad Anwer, and Fahad Shahbaz Khan. EdgeNeXt: Efficiently Amalgamated CNN-Transformer Architecture for Mobile Vision Applications. In Leonid Karlinsky, Tomer Michaeli, and Ko Nishino, editors, *Computer Vision – ECCV 2022 Workshops*, Lecture Notes in Computer Science, pages 3–20, Cham, 2023.
- [43] Sachin Mehta and Mohammad Rastegari. Mobilevit: Light-weight, general-purpose, and mobile-friendly vision transformer. In *International Conference on Learning Representations*, 2022.
- [44] Sachin Mehta and Mohammad Rastegari. Separable Self-attention for Mobile Vision Transformers, June 2022.
- [45] Julian Moosmann, Marco Giordano, Christian Vogt, and Michele Magno. Tinyissimoyolo: A quantized, low-memory footprint, tinymml object detection network for low power microcontrollers. In *2023 IEEE 5th International Conference on Artificial Intelligence Circuits and Systems (AICAS)*, pages 1–5, 2023.
- [46] Yali Nie, Paolo Sommella, Mattias O’Nils, Consolatina Liguori, and Jan Lundgren. Automatic detection of melanoma with yolo deep convolutional neural networks. In *2019 E-Health and Bioengineering Conference (EHB)*, pages 1–4. IEEE, 2019.
- [47] Dinh-Lam Pham, Tai-Woo Chang, et al. A yolo-based real-time packaging defect detection system. *Procedia Computer Science*, 217:886–894, 2023.

- [48] Isabel Pinheiro, Germano Moreira, Daniel Queirós da Silva, Sandro Magalhães, António Valente, Paulo Moura Oliveira, Mário Cunha, and Filipe Santos. Deep learning yolo-based solution for grape bunch detection and assessment of biophysical lesions. *Agronomy*, 13(4):1120, 2023.
- [49] Nitin Rane. Yolo and faster r-cnn object detection for smart industry 4.0 and industry 5.0: applications, challenges, and opportunities. Available at SSRN 4624206, 2023.
- [50] Joseph Redmon, Santosh Divvala, Ross Girshick, and Ali Farhadi. You only look once: Unified, real-time object detection. In *Proceedings of the IEEE Conference on Computer Vision and Pattern Recognition (CVPR)*, pages 779–788, June 2016.
- [51] Joseph Redmon and Ali Farhadi. Yolo9000: Better, faster, stronger. In *Proceedings of the IEEE Conference on Computer Vision and Pattern Recognition (CVPR)*, July 2017.
- [52] Joseph Redmon and Ali Farhadi. Yolov3: An incremental improvement. *arXiv preprint arXiv:1804.02767*, 2018.
- [53] Shaoqing Ren, Kaiming He, Ross Girshick, and Jian Sun. Faster r-cnn: Towards real-time object detection with region proposal networks. *Advances in neural information processing systems*, 28, 2015.
- [54] Mark Sandler, Andrew Howard, Menglong Zhu, Andrey Zhmoginov, and Liang-Chieh Chen. Mobilenetv2: Inverted residuals and linear bottlenecks. In *Proceedings of the IEEE conference on computer vision and pattern recognition*, pages 4510–4520, 2018.
- [55] Thiago T. Santos, Leonardo L. de Souza, Andreza A. dos Santos, and Sandra Avila. Grape detection, segmentation, and tracking using deep neural networks and three-dimensional association. *Computers and Electronics in Agriculture*, 170:105247, March 2020.
- [56] Marco Sozzi, Silvia Cantalamessa, Alessia Cogato, Ahmed Kayad, and Francesco Marinello. Automatic Bunch Detection in White Grape Varieties Using YOLOv3, YOLOv4, and YOLOv5 Deep Learning Algorithms. *Agronomy*, 12(2):319, 2022.
- [57] Christian Szegedy, Sergey Ioffe, Vincent Vanhoucke, and Alexander Alemi. Inception-v4, Inception-ResNet and the Impact of Residual Connections on Learning. *Proceedings of the AAAI Conference on Artificial Intelligence*, 31(1), February 2017.
- [58] Christian Szegedy, Wei Liu, Yangqing Jia, Pierre Sermanet, Scott Reed, Dragomir Anguelov, Dumitru Erhan, Vincent Vanhoucke, and Andrew Rabinovich. Going Deeper With Convolutions. pages 1–9, 2015.
- [59] Christian Szegedy, Vincent Vanhoucke, Sergey Ioffe, Jon Shlens, and Zbigniew Wojna. Rethinking the inception architecture for computer vision. In *Proceedings of the IEEE conference on computer vision and pattern recognition*, pages 2818–2826, 2016.
- [60] Lu Tan, Tianran Huangfu, Liyao Wu, and Wenying Chen. Comparison of RetinaNet, SSD, and YOLO v3 for real-time pill identification. *BMC Medical Informatics and Decision Making*, 21(1):324, November 2021.
- [61] Mingxing Tan, Bo Chen, Ruoming Pang, Vijay Vasudevan, Mark Sandler, Andrew Howard, and Quoc V. Le. MnasNet: Platform-Aware Neural Architecture Search for Mobile. In *2019 IEEE/CVF Conference on Computer Vision and Pattern Recognition (CVPR)*, pages 2815–2823, Long Beach, CA, USA, June 2019.
- [62] Mingxing Tan and Quoc Le. EfficientNet: Rethinking Model Scaling for Convolutional Neural Networks. In *Proceedings of the 36th International Conference on Machine Learning*, pages 6105–6114. PMLR, May 2019.
- [63] Mingxing Tan and Quoc Le. EfficientNetV2: Smaller Models and Faster Training. In *Proceedings of the 38th International Conference on Machine Learning*, pages 10096–10106. PMLR, July 2021.
- [64] Mingxing Tan, Ruoming Pang, and Quoc V Le. Efficientdet: Scalable and efficient object detection. In *Proceedings of the IEEE/CVF conference on computer vision and pattern recognition*, pages 10781–10790, 2020.

- [65] Yehui Tang, Kai Han, Jianyuan Guo, Chang Xu, Chao Xu, and Yunhe Wang. GhostNetV2: Enhance Cheap Operation with Long-Range Attention. *Advances in Neural Information Processing Systems*, 35:9969–9982, December 2022.
- [66] Naftali Tishby and Noga Zaslavsky. Deep learning and the information bottleneck principle. In *2015 IEEE Information Theory Workshop (ITW)*, pages 1–5, April 2015.
- [67] Halil Murat Ünver and Enes Ayan. Skin lesion segmentation in dermoscopic images with combination of yolo and grabcut algorithm. *Diagnostics*, 9(3):72, 2019.
- [68] Pavan Kumar Anasosalu Vasu, James Gabriel, Jeff Zhu, Oncel Tuzel, and Anurag Ranjan. Fastvit: A fast hybrid vision transformer using structural reparameterization. In *Proceedings of the IEEE/CVF International Conference on Computer Vision*, pages 5785–5795, 2023.
- [69] Pavan Kumar Anasosalu Vasu, James Gabriel, Jeff Zhu, Oncel Tuzel, and Anurag Ranjan. Mobileone: An improved one millisecond mobile backbone. In *Proceedings of the IEEE/CVF conference on computer vision and pattern recognition*, pages 7907–7917, 2023.
- [70] Shakti N Wadekar and Abhishek Chaurasia. Mobilevitv3: Mobile-friendly vision transformer with simple and effective fusion of local, global and input features. *arXiv preprint arXiv:2209.15159*, October 2022.
- [71] Chien-Yao Wang, Alexey Bochkovskiy, and Hong-Yuan Mark Liao. Yolov7: Trainable bag-of-freebies sets new state-of-the-art for real-time object detectors. In *Proceedings of the IEEE/CVF Conference on Computer Vision and Pattern Recognition (CVPR)*, pages 7464–7475, June 2023.
- [72] Chien-Yao Wang, Hong-Yuan Mark Liao, Yueh-Hua Wu, Ping-Yang Chen, Jun-Wei Hsieh, and I-Hau Yeh. Cspnet: A new backbone that can enhance learning capability of cnn. In *Proceedings of the IEEE/CVF conference on computer vision and pattern recognition workshops*, pages 390–391, 2020.
- [73] Chien-Yao Wang, I-Hau Yeh, and Hong-Yuan Mark Liao. Yolov9: Learning what you want to learn using programmable gradient information. *arXiv preprint arXiv:2402.13616*, 2024.
- [74] Fangxin Wang, Miao Zhang, Xiangxiang Wang, Xiaoqiang Ma, and Jiangchuan Liu. Deep Learning for Edge Computing Applications: A State-of-the-Art Survey. *IEEE Access*, 8:58322–58336, 2020.
- [75] Zixuan Wang, Jiacheng Zhang, Zhicheng Zhao, and Fei Su. Efficient Yolo: A Lightweight Model For Embedded Deep Learning Object Detection. In *2020 IEEE International Conference on Multimedia & Expo Workshops (ICMEW)*, pages 1–6, July 2020.
- [76] Wang Yang, Ding BO, and Li Su Tong. TS-YOLO: An efficient YOLO Network for Multi-scale Object Detection. In *2022 IEEE 6th Information Technology and Mechatronics Engineering Conference (ITOEC)*, volume 6, pages 656–660, March 2022.
- [77] Xiangyu Zhang, Xinyu Zhou, Mengxiao Lin, and Jian Sun. Shufflenet: An extremely efficient convolutional neural network for mobile devices. In *Proceedings of the IEEE conference on computer vision and pattern recognition*, pages 6848–6856, 2018.
- [78] Zixiao Zhang, Xiaoqiang Lu, Guojin Cao, Yuting Yang, Licheng Jiao, and Fang Liu. ViT-YOLO: Transformer-Based YOLO for Object Detection. In *2021 IEEE/CVF International Conference on Computer Vision Workshops (ICCVW)*, pages 2799–2808, October 2021.
- [79] Hengshuang Zhao, Jianping Shi, Xiaojuan Qi, Xiaogang Wang, and Jiaya Jia. Pyramid scene parsing network. In *Proceedings of the IEEE conference on computer vision and pattern recognition*, pages 2881–2890, 2017.
- [80] Zhi Zhou, Xu Chen, En Li, Liekang Zeng, Ke Luo, and Junshan Zhang. Edge Intelligence: Paving the Last Mile of Artificial Intelligence With Edge Computing. *Proceedings of the IEEE*, 107(8):1738–1762, August 2019.

A Appendix / supplemental material

B Notations

Throughout the document, we use several notations to describe the essential components of deep learning, particularly in object detection—for example, the spatial size of different tensors described as P_i . This chapter covers all the notations used in the paper. Since there is little to no consensus on Deep Learning notations, we found it relevant to describe them in more depth in the appendix for readers who need further explanation.

To start, we want to provide more explanation on the main component of this paper: the computation formula. Throughout the paper, we consistently use the **FLOP** (Floating Point Operations) metric to compare our work with other state-of-the-art neural networks. By basing computations on the number of multiplications and additions required for the neural network, we establish a solid foundation for efficient model comparisons. The FLOP metric remains reliable regardless of the hardware used, making it a good indicator of computational efficiency. Although we could use other metrics such as speed, these are highly dependent on factors like neural network architecture parallelization, the hardware used, the accelerator software (TensorRT, CoreML, TFLite), and memory usage and transfer speeds.

The second main element we consistently use throughout the paper is **mAP** (mean Average Precision). Researchers widely use this metric to compare object detection-based neural networks. mAP measures the precision of the model by evaluating the overlap between the proposed bounding boxes and the actual annotated bounding boxes. While some papers compare models using mAP at a fixed threshold of 50% overlap (mAP50), we primarily use mAP50-95. This metric averages the precision over different overlap thresholds, ranging from 50% to 95%, covering a broader range of evaluation criteria.

In object detection, where the spatial size of the feature map is essential, we define P_i as the feature map size of our deep neural network. The sizes range from P_0 (640x640 pixels) to P_5 (20x20 pixels) for LeYOLO-Small to Medium, with i representing the number of strides used. Similarly, P_{i-1} denotes the size of the preceding feature map for the explicitly described feature map i .

Similarly, when describing hidden layers in the neural network, we refer to the entire block rather than a single convolution. For example, the paper describes a single inverted bottleneck as one hidden layer h_i that consists of two pointwise convolutions and one depthwise convolution. Throughout the paper, this lets us directly refer to the preceding inverted bottleneck as h_{i-1} .

Note that we might combine all notations to highlight specific components of the architecture. For instance, we denote the number of channels C at each semantic level P as C_{P_i} . We specify the height and width of the feature map for each semantic level P_i as H_{P_i} and W_{P_i} .

B.1 Complete State-of-the-art

This section provides a comprehensive comparison of the state-of-the-art, juxtaposing LeYOLO with YOLO mainline models, micro neural networks designed for object detection, and the leading classification model, SSDLite, operating at 320x320 resolution.

We evaluate our performance against others using two primary metrics: Mean Average Precision (mAP) and FLOPs. The mAP is computed with various parameters, including an IOU of 0.5. For FLOP however, the intertwined nature of MAC and FLOP formulas has resulted in inconsistencies, with researchers erroneously labeling their models using FLOP instead of MAC. This implies that the computational cost of the model is at least twice the stated initial amount.

We also added the number of parameters used in a lightweight state-of-the-art model for object detection. Except for impressive results from YOLOv9-Tiny with two million parameters, our contributions use very few parameters compared to others. Table 4 shows all results.

B.2 Overall Architecture

For the sake of readability, we have omitted a discussion of the semantic sharing strategy in the neck. We employ lightweight blocks for upsampling the feature map in the bottom-up pathway, while the

Table 4: State-of-the-art lightweight object detector.

Models	Input Size	mAP	mAP50	mAP75	S	M	L	FLOP(G)	Parameters (M)
MobileNetv3-S[25]	320	16.1	-	-	-	-	-	0.32	1.77
MobileNetv2-x0.5[54]	320	16.6	-	-	-	-	-	0.54	1.54
MnasNet-x0.5[61]	320	18.5	-	-	-	-	-	0.58	1.68
LeYOLO-Nano	320	25.2	37.7	26.4	5.5	23.7	48.0	0.66	1.1
MobileNetv3[24]	320	22	-	-	-	-	-	1.02	3.22
YOLOX-Nano[14]	320	25.3	-	-	-	-	-	1.08	0.91
NanoDet		23.5	-	-	-	-	-	1.2	0.95
LeYOLO-Small	320	29	42.9	30.6	6.5	29.1	53.4	1.126	1.9
LeYOLO-Nano	480	31.3	46	33.2	10.5	33.1	52.7	1.47	1.1
MobileNetv2[54]	320	22.1	-	-	-	-	-	1.6	4.3
MnasNet[61]	320	23	-	-	-	-	-	1.68	4.8
LeYOLO-Small	480	35.2	50.5	37.5	13.3	38.1	55.7	2.53	1.9
Tinier-YOLO		17	34	15.7	4.8	17.3	26.8	2.563	-
MobileNetv1[25]	320	22.2	-	-	-	-	-	2.6	5.1
LeYOLO-Medium	480	36.4	52.0	38.9	14.3	40.1	58.1	3.27	2.4
LeYOLO-Small	640	38.2	54.1	41.3	17.6	42.2	55.1	4.5	1.9
YOLOv5-n[30]	640	28	45.7	-	-	-	-	4.5	1.9
EfficientDet-D0[64]	512	33.80	52.2	35.8	12	38.3	51.2	5	3.9
LeYOLO-Medium	640	39.3	55.7	42.5	18.8	44.1	56.1	5.8	1.9
YOLOv7-Tiny[71]	416	33.3	49.9	-	-	-	-	5.8	6.2
YOLOX-Tiny[14]	416	32.8	50.3	-	-	-	-	6.5	5.06
YOLOv4-tiny[2]	-	21.7	-	-	-	-	-	6.96	6.06
YOLOv9-Tiny[73]	640	38.3	53.1	41.3	-	-	-	7.7	2
LeYOLO-Large	768	41	57.9	44.3	21.9	46.1	56.8	8.4	2.4
YOLOv6-N[32]	640	35.9	51.2	-	-	-	-	11.1	4.3

top-down pathway utilizes standard convolutions. Despite their pronounced cost, strided standard convolutions prove efficient in this context due to the low spatial size and the restrained number of channels used.

We experimented with inverted bottlenecks instead of convolutions but found them more costly and less accurate. Additionally, we refrain from using any convolutions before the first 20x20 upsampling, diverging from the approach taken in most YOLO architectures. We question the necessity of another convolution after the Spatial Pyramid Pooling Fusion (SPPF) [30, 29], as it may already be sufficiently efficient in the backbone. Lastly, the 80x80 aspect is resource-intensive and requires careful consideration. Following similar reasoning, we avoided computation for the 80x80 top-down pathway, as the cost seemed disproportionate to the marginal accuracy improvement, as demonstrated in ablation studies on FPNets’s 80x80 pointwise component. Figure 6 represents the complete architecture of LeYOLO.

B.3 Architecture differences

We propose a comparison between our proposition and several inverted bottleneck-inspired backbones. Despite being disregarded by most contemporary state-of-the-art object detectors, MobileNetv2 [54], MobileNetv3 [24], and EfficientNets [75, 63, 64] share the philosophy of employing inverted bottlenecks for object detection.

As mentioned in the introduction, advancements in GPUs have enabled the development of powerful and rapid neural networks. However, inverted bottlenecks provide limited depth for parallelizing multiple computation blocks. Parallelizing deep neural networks on embedded devices remains challenging, but there is optimism for the future. Research primarily focuses on reducing MAC and FLOP costs and occasionally even memory access costs. Naturally, execution speed remains a significant concern. Nevertheless, we aim to briefly compare our backbone (Table 5) using consistent notation with models that exhibit "similar" architecture (Tables 6, 7 and 8), particularly those utilizing inverted bottlenecks.

Through this comparison, we can observe the stride inverted bottleneck strategy. Upon code verification, we indeed notice a contrast in channel expansion when transitioning from one layer ($h_i; P_i$) to another ($h_{i+1}; P_{i+1}$) with a stride greater than one. Additionally, most inverted bottlenecks utilize an

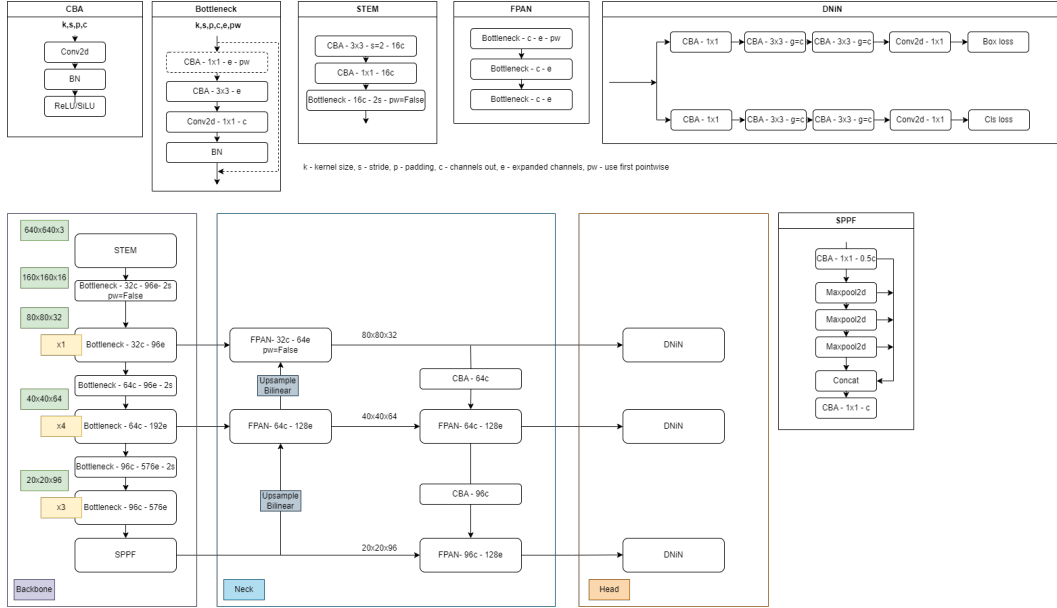


Figure 6: We present a visual decomposition of the LeYOLO network’s comprehensive architecture, providing a detailed explanation of its backbone, neck, and head components.

Table 5: LeYOLO backbone (base scale : nano).

Input	Operator	exp size	out size	NL	s
P0	conv2d, 3x3	-	16	SI	2
P1	conv2d, 1x1	16	16	SI	1
P1	bneck, 3x3, pw=False	16	16	SI	2
P2	bneck, 3x3	96	32	SI	2
P3	bneck, 3x3	96	32	SI	1
P3	bneck, 5x5	96	64	SI	2
P4	bneck, 5x5	192	64	SI	1
P4	bneck, 5x5	192	64	SI	1
P4	bneck, 5x5	192	64	SI	1
P4	bneck, 5x5	192	64	SI	1
P4	bneck, 5x5	576	96	SI	2
P5	bneck, 5x5	576	96	SI	1
P5	bneck, 5x5	576	96	SI	1
P5	bneck, 5x5	576	96	SI	1
P5	bneck, 5x5	576	96	SI	1

expansion ratio of 6, whereas we only expand to 3 within a block. This reduces overall computation and allows the inverted bottleneck stride strategy to expand the number of channels one last time before the stride within the depthwise convolution.

Table 6: MobileNetv2 backbone.

Input	Operator	exp size	out size	NL	s
P0	conv2d, 3x3	-	32	RE	2
P1	bneck, 3x3	16	16	RE	1
P1	bneck, 3x3	96	24	RE	2
P2	bneck, 3x3	144	24	RE	1
P2	bneck, 3x3	144	32	RE	2
P3	bneck, 3x3	192	32	RE	1
P3	bneck, 3x3	192	32	RE	1
P3	bneck, 3x3	192	64	RE	2
P4	bneck, 3x3	384	64	RE	1
P4	bneck, 3x3	384	64	RE	1
P4	bneck, 3x3	384	64	RE	1
P4	bneck, 3x3	384	96	RE	1
P4	bneck, 3x3	576	96	RE	1
P4	bneck, 3x3	576	96	RE	1
P4	bneck, 3x3	576	160	RE	2
P5	bneck, 3x3	960	160	RE	1
P5	bneck, 3x3	960	320	RE	1
P5	conv, 1x1	1920	320	RE	1

Table 7: MobileNetv3 backbone.

Input	Operator	exp size	out size	NL	s
P0	conv2d, 3x3	-	16	HS	2
P1	conv2d, 1x1	16	16	RE	2
P2	bneck, 3x3	72	24	RE	2
P3	bneck, 3x3	88	24	RE	1
P3	bneck, 5x5	96	40	HS	2
P4	bneck, 5x5	96	40	HS	1
P4	bneck, 5x5	240	40	HS	1
P4	bneck, 5x5	240	40	HS	1
P4	bneck, 5x5	120	48	HS	1
P4	bneck, 5x5	144	48	HS	1
P4	bneck, 5x5	288	96	HS	2
P5	bneck, 5x5	576	96	HS	1
P5	bneck, 5x5	576	96	HS	1

Table 8: EfficientNet-B0 (EfficientDet-D0 and D1) backbone.

Input	Operator	exp size	out size	NL	s
P0	conv2d, 3x3	-	32	RE	2
P1	bneck, 3x3	16	16	RE	1
P1	bneck, 3x3	96	24	RE	2
P2	bneck, 3x3	144	24	RE	1
P2	bneck, 5x5	144	40	RE	2
P3	bneck, 5x5	240	40	RE	1
P3	bneck, 3x3	240	80	RE	1
P3	bneck, 3x3	480	80	RE	1
P3	bneck, 3x3	480	80	RE	1
P3	bneck, 5x5	480	112	RE	2
P4	bneck, 5x5	672	112	RE	1
P4	bneck, 5x5	672	112	RE	1
P4	bneck, 5x5	672	192	RE	2
P5	bneck, 5x5	1152	192	RE	1
P5	bneck, 5x5	1152	192	RE	1
P5	bneck, 5x5	1152	192	RE	1
P5	bneck, 3x3	1280	320	RE	1

B.4 Ablation study

It is difficult to mathematically prove universal truths, such as whether one neural network architecture performs better than another without training. However, we do not see this as a problem; on the contrary, we use ablation studies to prove that our architecture is functional. Moreover, we have encountered architectures that perform better than our final proposed contribution but require higher computational costs. This ablation study represents the most relevant experiments we have been able to carry out. However, we have left it to the reader to choose the most efficient, albeit more costly, to use them in future research to guide researchers more effectively.

B.4.1 Kernel size

Kernel filter size: For narrative clarity, we directly outline the final architecture selected for optimal accuracy and FLOP efficiency in the paper. However, our study began with a minimalist architecture based on an inverted bottleneck. Initially, we experimented with kernel sizes of 5x5 and 7x7 when the feature map size reached 80x80. Our ablation study revealed that a larger kernel size yields promising results, as indicated in Table 9. Although the 7x7 kernel outperforms 3x3 (+2,4 mAP points) and 5x5 (+0.4 mAP points), it significantly increases FLOP requirements. Therefore, we opted for the 5x5 kernel to balance FLOP utilization and accuracy.

Kernel size ablation study:

1. minimal: minimal architecture with classic inverted bottleneck and full 3x3 convolutions
2. 5x5 : minimal architecture with 5x5 convolutions at and after P3.
3. 7x7 : minimal architecture with 7x7 convolutions at and after P3.

With **34.9 mAP** on MSCOCO and **3,293 FLOP(G)**, the best choice was to use a consistent **5x5** kernel size throughout the model from semantic level P3 to P5 (Stem remains with a 3x3 kernel size).

Kernel size and feature map size cost: The P3 (80x80) feature map incurs considerable computational costs, necessitating a reduction in computation at this model stage. One objective is optimizing model efficiency by exclusively employing 5x5 convolutions from P4 to P5 instead of P3 to P5 along the backbone and FPANet.

Moreover, the effectiveness of employing two convolutions at 5x5 with a stride of two in the top-down pathway of the FPANet still needs to be proven. We explored the efficacy of different kernel sizes by employing 3x3 convolutions for downsampling in the FPANet. Our ablation study identified the optimal compromise for kernel size at this juncture, as illustrated in Table 9.

Kernel size ablation study:

1. 5x5@P4 : minimal architecture with 5x5 convolutions at and after P4.
2. FPANet 3x3 ↓ : minimal architecture with **5x5@P4** and only 3x3 convolutions for downsampling in FPANet

Regarding the mAP to FLOP ratio, we observed a better kernel filter size choice by combining the use of 5x5 kernel size from P4 to P5 (with Stem and P3 using a consistent 3x3 kernel size) and the use of 3x3 kernel size for FPANet downsampling convolutions. These choices pushed the mAP to FLOP ratio to $\frac{mAP}{FLOP(G)} = 11,49$ with **34,6 mAP** for **3,011 FLOP(G)**

B.4.2 Architecture improvement

To improve the architecture, we aimed to simplify all computations before P4. Having already made adjustments regarding kernel size at P3, we removed the initial pointwise operation in the STEM at P2 (160x160), as the input channel matched the number of required channels for the depthwise convolution. Leveraging the efficiency of our inverted bottleneck building block, coupled with optional pointwise operations, unexpectedly improved the model with **34,7 mAP** and reduced computation by 66MFLOP (**2,945 FLOP(G)**).

In line with this optimization process, we opted for a channel configuration in both the minimal and final architectures, aligned with a compressed information bottleneck $I(h_1; h_n)$ (Equation (6)),

limiting input channels at each block. In this manner, the feature map concatenation from the bottom-up pathway of P4 C_{out} and P3 C_{out} , retained in memory from the backbone, already matched the desired expanded channel number for the P3 block C_{mid} in the FPANet. Thus, we streamlined the architecture to its essential components before P4, freeing up computation resources for an impressive **34.1 mAP for 2,823 FLOP(G)**.

Table 9 describes all results.

Minimal architecture improvement:

1. $no_{pw}@STEM$: no pointwise in the stem in the first inverted bottleneck at P1.
2. $no_{pw}@FPAN - P3$: no pointwise in the first inverted bottleneck at P3 in the bottom-up FPAN pathway.

While some studies may advocate retaining the previous configuration, arguing that removing pointwise convolutions compromises accuracy, we pursued alternative experiments to improve the accuracy to FLOP ratio. Despite the potential controversy, we maintain the integrity of our ablation study, preserving all findings for the benefit of researchers or readers who may find value in various aspects of our experimentation.

Table 9: Ablation study on minimal inverted bottleneck architecture.

minimal	5x5	7x7	5x5@P4	FPANet 3x3 ↓	$no_{pw}@STEM$	$no_{pw}@FPAN - P3$	mAP	FLOP(G)
✓	-	-	-	-	-	-	32,9	2,877
-	✓	-	-	-	-	-	34,9	3,293
-	-	✓	-	-	-	-	35,3	3,946
-	-	-	✓	-	-	-	34,2	3,19
-	-	-	✓	✓	-	-	34,6	3,011
-	-	-	✓	✓	✓	-	34,7	2,945
-	-	-	✓	✓	✓	✓	34,1	2,823

B.4.3 Channels choice

We aimed to determine the optimal number of channels without resorting to costly training algorithms like NAS, relying instead on iterative experimentation based on previous architecture choices. Consequently, we conducted various experiments, including exploring the ideal number of channels within the FPANet. Table 10 describes all the following explanations.

Backbone channels choice: We desired to optimize channel selection and discovered that expanding information from P3 to P4 by a factor of 3 rather than 6, while less potent, required less computation. In this experimentation, we kepted the strided inverted bottleneck channels expansion ratio of 6 in between P2 to P3 (from 16 $C_{in}P_2$ channels to 96 $C_{mid}P_3$) and P4 to P5 (from 64 $C_{in}P_4$ to 576 $C_{mid}P_5$ channels for LeYOLO-Nano base channels choice).

Neck channels choice: Exemplified by our consistent expansion channel choice of 3 throughout all the models, we tested different expansion ratios inside the neck with an expansion ratio of 2 and 2.5. With these experimentations, we wanted to compare the benefits of adding more expansion channels in the backbone or the neck. Regarding our choices, we compare the neural network’s performance with more support on the backbone at P5, exemplified by an expansion ratio of 6, and less pressure on the neck, exemplified by an expansion ratio of 2 instead of 3 within the whole FPAN neck.

Looking at the ablation proposed in Table 10, we observe that globally, simplifying the number of channels inside the neck with an expansion ratio of 2 was the better choice as the greater expansion strategy inside the bottleneck at P5 led to better accuracy and mAP to FLOP ratio.

Channel choice:

1. CC : Channel choice - we reduce the expansion ratio from P3 to P4 to 3 instead of 6.
2. CCx6 : We augment the expansion ratio inside P5 for all block to 6 instead of 3.
3. FPANx2 : All FPAN inverted bottleneck block use a ratio of 2 instead of 3.
4. FPANx2.5 : All FPAN inverted bottleneck block use a ratio of 2.5 instead of 3.

Table 10: Ablation study on channels choice improvement.

$no_{pw}@STEM$	$no_{pw}@FPAN - P3$	CC	CCx6	FPANx2	FPANx2.5	mAP	FLOP(G)
✓	✓	✓	-	-	-	33,5	2,75
✓	✓	✓	-	✓	-	32,3	2,39
✓	✓	✓	-	-	✓	32,9	2,573
✓	✓	-	-	✓	-	32.6	2,467
✓	✓	-	✓	✓	-	33,7	2,714
✓	✓	✓	✓	✓	-	34.3	2,64

Table 11: LeYOLO base training scaling architecture with their respective results

Models	Nano	Small	Medium	Large
Input spatial size	640	640	640	768
Channels ratio	x1	x1.33	x1.33	x1.33
Layer ratio	x1	x1	x1.33	x1.33
mAP	34.3	38.2	39.3	41

Regarding the initial minimal architecture chosen for experimentation, we began with a 32.9 mAP at 2.877 GFLOP. Following iterative refinements validated through training experiments, we boosted the accuracy to **34.3 mAP** while reducing computational requirements to **2.64 GFLOP** for LeYOLO-Nano. This signifies an enhancement in accuracy alongside a reduction in computational complexity during the model refinement process.

B.4.4 Architecture scaling choice

This section provides more insight into the model scaling proposed in our contributions. As discussed in the chapter 2.6.1, we propose four different scaling methods, compressing the architecture below 10 FLOP(G). Table 11 illustrates the four training scaling possibilities (Nano to Large), and Table 12 shows the eight final proposed scaling for inferences.

Table 12: Architecture scaling with different parameter multipliers.

Models	Nano	Nano	Small	Small	Small	Medium	Medium	Large
Input spatial size	320p	480p	320p	480p	640p	480p	640p	768p
Channels ratio	x1	x1	x1.33	x1.33	x1.33	x1.33	x1.33	x1.33
Layer ratio	x1	x1	x1	x1	x1	x1.33	x1.33	x1.33

We can effectively transfer the core architecture from the previously mentioned ablation study to different input sizes during inference and validation. For instance, a neural network explicitly trained at 640p might yield better results when compressed and validated at 320p than a neural network trained from scratch at 320p. Consequently, we tested various scales of LeYOLO—Nano, Small, Medium, and Large trained neural network from Table 11—to determine the optimal input and training combinations. The results presented in Table 13 highlight the best outcomes from this study.

B.4.5 Speed tests

As discussed in the paper, we proposed a highly efficient family of neural network models, focusing solely on FLOP computation and disregarding execution speed. Inverted bottlenecks inherently reduce the parallelization potential of the neural network, causing GPUs to wait for subsequent operations sequentially. Consequently, while our models may not be the fastest in the state-of-the-art, they offer various models with varying execution speeds. We focus on object detectors on embedded devices, so we propose a comparison using a 4GB Jetson TX2 coupled with the TensorRT software accelerator to observe the state-of-the-art parallelization capability. We can find details of execution speed, accuracy, query per second, FLOP, and qps in Table 14 and Figure 7.

Table 13: Ablation study on best training and validation input size

Models	training dim	validation dim	mAP	FLOP(G)
LeYOLO-Nano	320	320	24.1	0.66
LeYOLO-Nano	640	320	25.2	0.66
LeYOLO-Nano	480	480	30.9	1.47
LeYOLO-Nano	640	480	31.3	1.47
LeYOLO-Nano(ablation study)	640	640	34.3	2.65
LeYOLO-Small	640	320	29.0	1.126
LeYOLO-Small	640	480	35.2	2.53
LeYOLO-Small	640	640	38.2	4.51
LeYOLO-Medium	640	320	30.0	1.45
LeYOLO-Medium	640	480	36.4	3.27
LeYOLO-Medium	640	640	39.3	5.8
LeYOLO-Large	768	768	41	8.4

Table 14: Execution speed of reproducible YOLOs and our contribution (sorted by queries per second).

Models	QPS	FLOP(G)	mAP(%)
LeYOLO-Nano@320	99.56	0.66	25.2
LeYOLO-Small@320	75.36	1.126	29
LeYOLO-Nano@480	51.39	1.47	31.3
LeYOLO-Small@480	39.29	2.53	35.2
YOLOv5n	38	4.5	28
YOLOv6n	37.935	11.1	35.9
YOLOv8n	33.650	8.7	37.3
LeYOLO-Medium@480	32.83	3.27	36.4
YOLOv7-Tiny	24.8	5.8	33.3
LeYOLO-Small@640	24	4.5	38.2
LeYOLO-Medium@640	19.89	5.8	39.3
YOLOX-s	14.6	26.8	40.5
LeYOLO-Large@768	14.2	8.4	41

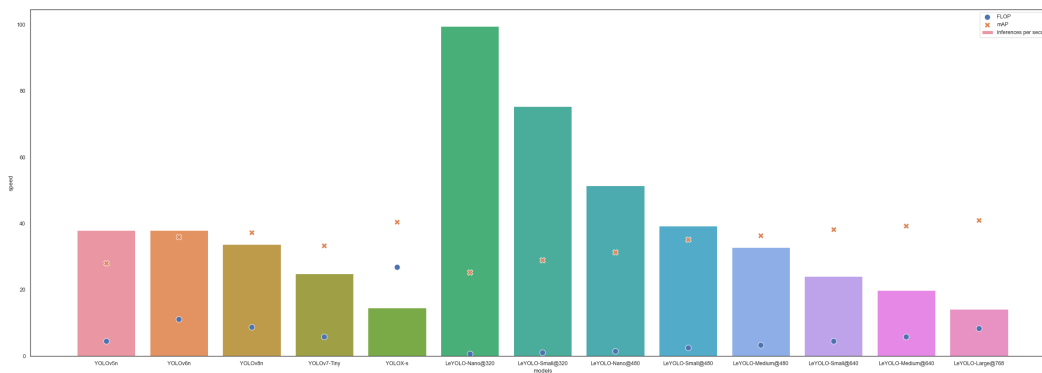


Figure 7: YOLO and LeYOLO speed comparison on Jetson TX2 coupled with TensorRT.

B.5 Code

As we could use PyTorch, Tensorflow, or any other API, we are using the Ultralytics code on the YOLOv8 version to develop our version of LeYOLO. Using these tools and implementing the code will be simple, centralizing research on a single tool.

```
class mn_conv(nn.Module):
    #Cin, Cout, Kernel, stride, padding, group, dilation
    def __init__(self, c1, c2, k=1, s=1, p=None, g=1, d=1):
        super().__init__()
        #autopad -> ultralytics and YOLOv9 auto select padding
        #regarding kernel size and
        #dilation
        padding = 0 if k==s else autopad(k,p,d)
        self.c = nn.Conv2d(c1, c2, k, s, padding, groups=g)
        self.bn = nn.BatchNorm2d(c2)
        self.act = nn.SiLU()

    def forward(self, x):
        return self.act(self.bn(self.c(x)))

class InvertedBottleneck(nn.Module):
    #Cin, Cout, kernel size, expansion number (Cin*3 most of the time)
    #stride, first poinwise
    def __init__(self, c1, c2, k=3, e=None, stride=1, pw=True):
        #input_channels, output_channels, repetition, stride,
        #expansion ratio
        super().__init__()
        c_mid = e if e != None else c1
        self.residual = c1 == c2 and stride == 1

        features = [mn_conv(c1, c_mid, act=act)] if pw else []
        features.extend([
            mn_conv(c_mid, c_mid, k, stride, g=c_mid, act=
                act),
            nn.Conv2d(c_mid, c2, 1),
            nn.BatchNorm2d(c2),
        ])
        self.layers = nn.Sequential(*features)
    def forward(self, x):
        if self.residual:
            return x + self.layers(x)
        else:
            return self.layers(x)
```

```

class Detect(nn.Module):
    """LeYOLO Detect head for detection models."""

    dynamic = False
    export = False
    shape = None
    anchors = torch.empty(0) # init
    strides = torch.empty(0) # init

    def __init__(self, nc=80, ch=()):
        super().__init__()
        self.nc = nc
        self.nl = len(ch)
        self.reg_max = 16
        self.no = nc + self.reg_max * 4
        self.stride = torch.zeros(self.nl)

        c2, c3 = max((16, ch[0] // 4, self.reg_max * 4), max(ch[0],
                                                             min(self.nc, 100)))

        self.cv2 = nn.ModuleList(
            nn.Sequential(Conv(x, c2, 1),
                          Conv(c2, c2, 3, g=c2), Conv(c2, c2, 3, g=c2),
                          nn.Conv2d(c2, 4 * self.reg_max, 1)) for x in ch
        )
        self.cv3 = nn.ModuleList(
            nn.Sequential(Conv(x, c3, 1),
                          Conv(c3, c3, 3, g=c3), Conv(c3, c3, 3, g=c3),
                          nn.Conv2d(c3, self.nc, 1)) for x in ch
        )

        self.dfl = DFL(self.reg_max) if self.reg_max > 1 else nn.
            Identity()

    def forward(self, x):

        """Concatenates and returns predicted bounding boxes and class
        probabilities."""
        for i in range(self.nl):
            x[i] = torch.cat((self.cv2[i](x[i]),
                              self.cv3[i](x[i])), 1)
            if self.training: # Training path
                return x

            # Inference path
            shape = x[0].shape # BCHW
            x_cat = torch.cat([
                xi.view(shape[0], self.no, -1) for xi in x
            ], 2)
            if self.dynamic or self.shape != shape:
                self.anchors, self.strides = (x.transpose(0, 1)
                                               for x in make_anchors(x, self.stride, 0.5))
                self.shape = shape

            dbox = self.decode_bboxes(box)

            y = torch.cat((dbox, cls.sigmoid()), 1)
            return y if self.export else (y, x)

```

```

def decode_bboxes(self, bboxes):
    """Decode bounding boxes."""
    return dist2bbox(self.dfl(bboxes),
                    self.anchors.unsqueeze(0), xywh=True, dim=1)
    * self.strides

def dist2bbox(distance, anchor_points, xywh=True, dim=-1):
    """Transform distance(ltrb) to box(xywh or xyxy)."""
    lt, rb = distance.chunk(2, dim)
    x1y1 = anchor_points - lt
    x2y2 = anchor_points + rb
    if xywh:
        c_xy = (x1y1 + x2y2) / 2
        wh = x2y2 - x1y1
        return torch.cat((c_xy, wh), dim) # xywh bbox
    return torch.cat((x1y1, x2y2), dim) # xyxy bbox

```

```

backbone:
# [from, repeats, module, args]
- [-1, 1, mn_conv, [16, 3, 2]]
- [-1, 1, mn_conv, [16, 1, 1]]
- [-1, 1, InvertedBottleneck, [16, 3, 16, 2, False]]
- [-1, 1, InvertedBottleneck, [32, 3, 96, 2]]
- [-1, 1, InvertedBottleneck, [32, 3, 96, 1]]
- [-1, 1, InvertedBottleneck, [64, 5, 96, 2]]
- [-1, 1, InvertedBottleneck, [64, 5, 192, 1]]
- [-1, 1, InvertedBottleneck, [96, 5, 576, 2]]
- [-1, 1, InvertedBottleneck, [96, 5, 576, 1]]
- [-1, 1, InvertedBottleneck, [96, 5, 576, 1]]
- [-1, 1, InvertedBottleneck, [96, 5, 576, 1]]
- [-1, 1, SPPF, [96, 5]]

# LeYOLO FPNNet
head:
- [-1, 1, nn.Upsample, [None, 2, 'nearest']]
- [-1, 1, InvertedBottleneck, [64, 5, 128, 1]]
- [-1, 1, InvertedBottleneck, [64, 5, 128, 1]]
- [-1, 1, InvertedBottleneck, [64, 5, 128, 1]]

- [-1, 1, nn.Upsample, [None, 2, 'nearest']]
- [[-1, 4], 1, Concat, [1]]
- [-1, 1, InvertedBottleneck, [32, 3, 96, 1, False]]
- [-1, 1, InvertedBottleneck, [32, 3, 64, 1]]
- [-1, 1, InvertedBottleneck, [32, 3, 64, 1]]

- [-1, 1, mn_conv, [64, 3, 2]]
- [[-1, 19], 1, Concat, [1]]
- [-1, 1, InvertedBottleneck, [64, 5, 128, 1]]
- [-1, 1, InvertedBottleneck, [64, 5, 128, 1]]
- [-1, 1, InvertedBottleneck, [64, 5, 128, 1]]

- [-1, 1, mn_conv, [96, 3, 2]]
- [[-1, 14], 1, Concat, [1]]
- [-1, 1, InvertedBottleneck, [96, 5, 192, 1]]
- [-1, 1, InvertedBottleneck, [96, 5, 192, 1]]
- [-1, 1, InvertedBottleneck, [96, 5, 192, 1]]

#LeYOLO DNiN Head
- [[24, 29, 34], 1, Detect, [nc]] # Detect (P3, P4, P5)

```

B.6 Training specificity

Training on MSCOCO. We train our model on the MSCOCO dataset [37] using the standard data augmentation [49] with stochastic gradient descent (SGD) and batch size of 128 on four GPUs. Learning rate is initially set to 0.01 with a momentum set to 0.9. Weight decay is set to 0.001.

Mosaic data augmentation : throughout the training, we found through multiple experiments that there is minimal variation in accuracy attributable to Mosaic data augmentation. This phenomenon primarily arises from small objects with limited data samples, such as toothbrushes in MSCOCO, where Mosaic augmentation could potentially have adverse effects. Across our experiments, we noted a potential variance of 0.4 mAP.

1. epochs: 500
2. patience: 50
3. batch: 128
4. imgsz: 640
5. gpu count: 4
6. workers: 8
7. optimizer: SGD
8. seed: 0
9. close mosaic: 10
10. training iou: 0.7
11. max detections: 300
12. lr0: 0.01
13. lrf: 0.01
14. momentum: 0.9
15. weight decay: 0.001
16. warmup epochs: 3.0
17. warmup momentum: 0.8
18. warmup bias lr: 0.1
19. box: 7.5
20. cls: 0.5
21. dfl: 1.5
22. pose: 12.0
23. kobj: 1.0
24. label smoothing: 0.0
25. nbs: 64
26. hsv h: 0.015
27. hsv s: 0.7
28. hsv v: 0.4
29. degrees: 0.0
30. translate: 0.1
31. scale: 0.5
32. shear: 0.0
33. perspective: 0.0
34. flipud: 0.0
35. fliplr: 0.5

- 36. mosaic: 1.0
- 37. mixup: 0.0
- 38. copy paste: 0.0
- 39. erasing: 0.4
- 40. crop fraction: 1.0

NeurIPS Paper Checklist

1. Claims

Question: Do the main claims made in the abstract and introduction accurately reflect the paper's contributions and scope?

Answer: [Yes]

Justification: *The abstract and introduction clearly state the purpose of neural networks with low computational resources for embedded devices and support its interest and the interest of YOLO for the industry. The introduction includes evidence of a contribution by the results (accuracy, precision, state-of-the-art comparison) and the contribution limitations (fully discussed in the discussion section.)*

Guidelines:

- The answer NA means that the abstract and introduction do not include the claims made in the paper.
- The abstract and/or introduction should clearly state the claims made, including the contributions made in the paper and important assumptions and limitations. A No or NA answer to this question will not be perceived well by the reviewers.
- The claims made should match theoretical and experimental results, and reflect how much the results can be expected to generalize to other settings.
- It is fine to include aspirational goals as motivation as long as it is clear that these goals are not attained by the paper.

2. Limitations

Question: Does the paper discuss the limitations of the work performed by the authors?

Answer: [Yes]

Justification: *The paper demonstrates the robustness of certain results through an ablation study on specific datasets. In the discussion chapter, we openly acknowledge our contributions' limitations, addressing the flaws and what is missing. We also discuss the computational efficiency of the proposed algorithms, advancing the boundaries of the FLOP to mAP ratio. However, we admit that our contributions may require speed improvements, as they are not the fastest in the state-of-the-art.*

Guidelines:

- The answer NA means that the paper has no limitation while the answer No means that the paper has limitations, but those are not discussed in the paper.
- The authors are encouraged to create a separate "Limitations" section in their paper.
- The paper should point out any strong assumptions and how robust the results are to violations of these assumptions (e.g., independence assumptions, noiseless settings, model well-specification, asymptotic approximations only holding locally). The authors should reflect on how these assumptions might be violated in practice and what the implications would be.
- The authors should reflect on the scope of the claims made, e.g., if the approach was only tested on a few datasets or with a few runs. In general, empirical results often depend on implicit assumptions, which should be articulated.
- The authors should reflect on the factors that influence the performance of the approach. For example, a facial recognition algorithm may perform poorly when image resolution is low or images are taken in low lighting. Or a speech-to-text system might not be used reliably to provide closed captions for online lectures because it fails to handle technical jargon.
- The authors should discuss the computational efficiency of the proposed algorithms and how they scale with dataset size.
- If applicable, the authors should discuss possible limitations of their approach to address problems of privacy and fairness.
- While the authors might fear that complete honesty about limitations might be used by reviewers as grounds for rejection, a worse outcome might be that reviewers discover limitations that aren't acknowledged in the paper. The authors should use their best

judgment and recognize that individual actions in favor of transparency play an important role in developing norms that preserve the integrity of the community. Reviewers will be specifically instructed to not penalize honesty concerning limitations.

3. Theory Assumptions and Proofs

Question: For each theoretical result, does the paper provide the full set of assumptions and a complete (and correct) proof?

Answer: [NA]

Justification: *In Chapter 2.3.1, we provide theoretical ideas on the optimization and compression of neural networks, including the choice of layers and number of channels. In the context of deep learning, it is difficult today to mathematically prove the choice of the number of layers, channels, and parameters with solid and unbreakable proof. Nevertheless, we strive to use experimental proof with as many samples as possible and ablation study.*

Guidelines:

- The answer NA means that the paper does not include theoretical results.
- All the theorems, formulas, and proofs in the paper should be numbered and cross-referenced.
- All assumptions should be clearly stated or referenced in the statement of any theorems.
- The proofs can either appear in the main paper or the supplemental material, but if they appear in the supplemental material, the authors are encouraged to provide a short proof sketch to provide intuition.
- Inversely, any informal proof provided in the core of the paper should be complemented by formal proofs provided in appendix or supplemental material.
- Theorems and Lemmas that the proof relies upon should be properly referenced.

4. Experimental Result Reproducibility

Question: Does the paper fully disclose all the information needed to reproduce the main experimental results of the paper to the extent that it affects the main claims and/or conclusions of the paper (regardless of whether the code and data are provided or not)?

Answer: [Yes]

Justification: *Our contribution uses experiments and is reproducible in many ways. We provide a code to quickly launch our model. Also, our model's flexible architecture easily integrates with Ultralytics (YOLOv8) or YOLOv9 repository for training and inference purposes.*

Guidelines:

- The answer NA means that the paper does not include experiments.
- If the paper includes experiments, a No answer to this question will not be perceived well by the reviewers: Making the paper reproducible is important, regardless of whether the code and data are provided or not.
- If the contribution is a dataset and/or model, the authors should describe the steps taken to make their results reproducible or verifiable.
- Depending on the contribution, reproducibility can be accomplished in various ways. For example, if the contribution is a novel architecture, describing the architecture fully might suffice, or if the contribution is a specific model and empirical evaluation, it may be necessary to either make it possible for others to replicate the model with the same dataset, or provide access to the model. In general, releasing code and data is often one good way to accomplish this, but reproducibility can also be provided via detailed instructions for how to replicate the results, access to a hosted model (e.g., in the case of a large language model), releasing of a model checkpoint, or other means that are appropriate to the research performed.
- While NeurIPS does not require releasing code, the conference does require all submissions to provide some reasonable avenue for reproducibility, which may depend on the nature of the contribution. For example
 - (a) If the contribution is primarily a new algorithm, the paper should make it clear how to reproduce that algorithm.

- (b) If the contribution is primarily a new model architecture, the paper should describe the architecture clearly and fully.
- (c) If the contribution is a new model (e.g., a large language model), then there should either be a way to access this model for reproducing the results or a way to reproduce the model (e.g., with an open-source dataset or instructions for how to construct the dataset).
- (d) We recognize that reproducibility may be tricky in some cases, in which case authors are welcome to describe the particular way they provide for reproducibility. In the case of closed-source models, it may be that access to the model is limited in some way (e.g., to registered users), but it should be possible for other researchers to have some path to reproducing or verifying the results.

5. Open access to data and code

Question: Does the paper provide open access to the data and code, with sufficient instructions to faithfully reproduce the main experimental results, as described in supplemental material?

Answer: [Yes]

Justification: *We make our code available. As for the data, we are only working on MSCOCO for this study.*

Guidelines:

- The answer NA means that paper does not include experiments requiring code.
- Please see the NeurIPS code and data submission guidelines (<https://nips.cc/public/guides/CodeSubmissionPolicy>) for more details.
- While we encourage the release of code and data, we understand that this might not be possible, so “No” is an acceptable answer. Papers cannot be rejected simply for not including code, unless this is central to the contribution (e.g., for a new open-source benchmark).
- The instructions should contain the exact command and environment needed to run to reproduce the results. See the NeurIPS code and data submission guidelines (<https://nips.cc/public/guides/CodeSubmissionPolicy>) for more details.
- The authors should provide instructions on data access and preparation, including how to access the raw data, preprocessed data, intermediate data, and generated data, etc.
- The authors should provide scripts to reproduce all experimental results for the new proposed method and baselines. If only a subset of experiments are reproducible, they should state which ones are omitted from the script and why.
- At submission time, to preserve anonymity, the authors should release anonymized versions (if applicable).
- Providing as much information as possible in supplemental material (appended to the paper) is recommended, but including URLs to data and code is permitted.

6. Experimental Setting/Details

Question: Does the paper specify all the training and test details (e.g., data splits, hyperparameters, how they were chosen, type of optimizer, etc.) necessary to understand the results?

Answer: [Yes]

Justification: *We show all the settings used to train the model. We have mainly based our study on "simple" learning techniques to focus on neural network architectures, although we know the wide range of training possibilities. As a result, readers don't have to worry about complex training methods and hyperparameters, as we use the basic YOLO training parameters on versions 5, 8, and 9.*

Guidelines:

- The answer NA means that the paper does not include experiments.
- The experimental setting should be presented in the core of the paper to a level of detail that is necessary to appreciate the results and make sense of them.
- The full details can be provided either with the code, in appendix, or as supplemental material.

7. Experiment Statistical Significance

Question: Does the paper report error bars suitably and correctly defined or other appropriate information about the statistical significance of the experiments?

Answer: [Yes]

Justification: *During our experiments, we based the importance of our results on a rigorous comparison with the state of the art. To achieve this comparison, we have included diagrams, plots, and other information relevant to understanding the experiments, both in the paper and in the appendix.*

Guidelines:

- The answer NA means that the paper does not include experiments.
- The authors should answer "Yes" if the results are accompanied by error bars, confidence intervals, or statistical significance tests, at least for the experiments that support the main claims of the paper.
- The factors of variability that the error bars are capturing should be clearly stated (for example, train/test split, initialization, random drawing of some parameter, or overall run with given experimental conditions).
- The method for calculating the error bars should be explained (closed form formula, call to a library function, bootstrap, etc.)
- The assumptions made should be given (e.g., Normally distributed errors).
- It should be clear whether the error bar is the standard deviation or the standard error of the mean.
- It is OK to report 1-sigma error bars, but one should state it. The authors should preferably report a 2-sigma error bar than state that they have a 96% CI, if the hypothesis of Normality of errors is not verified.
- For asymmetric distributions, the authors should be careful not to show in tables or figures symmetric error bars that would yield results that are out of range (e.g. negative error rates).
- If error bars are reported in tables or plots, The authors should explain in the text how they were calculated and reference the corresponding figures or tables in the text.

8. Experiments Compute Resources

Question: For each experiment, does the paper provide sufficient information on the computer resources (type of compute workers, memory, time of execution) needed to reproduce the experiments?

Answer: [Yes]

Justification: *Although our contribution uses a more global comparison of the computational cost of a neural network (MAC and FLOP), we are concerned with the speed of execution of such a model around YOLO architectures. To do this, we are running our contribution on one embedded device: Jetson TX2 4GB. For the speed benchmark, we have indicated the hardware used.*

Guidelines:

- The answer NA means that the paper does not include experiments.
- The paper should indicate the type of compute workers CPU or GPU, internal cluster, or cloud provider, including relevant memory and storage.
- The paper should provide the amount of compute required for each of the individual experimental runs as well as estimate the total compute.
- The paper should disclose whether the full research project required more compute than the experiments reported in the paper (e.g., preliminary or failed experiments that didn't make it into the paper).

9. Code Of Ethics

Question: Does the research conducted in the paper conform, in every respect, with the NeurIPS Code of Ethics <https://neurips.cc/public/EthicsGuidelines?>

Answer: [Yes]

Justification: *The paper does not violate the requirements of the Code of Ethics. Also, we preserve anonymity in the paper and the provided codes.*

Guidelines:

- The answer NA means that the authors have not reviewed the NeurIPS Code of Ethics.
- If the authors answer No, they should explain the special circumstances that require a deviation from the Code of Ethics.
- The authors should make sure to preserve anonymity (e.g., if there is a special consideration due to laws or regulations in their jurisdiction).

10. **Broader Impacts**

Question: Does the paper discuss both potential positive societal impacts and negative societal impacts of the work performed?

Answer: [Yes]

Justification: *YOLO has a significant societal impact, especially in the edge, embedded, and industrial sectors. This is partly due to previous work enabling YOLO to be used rapidly by most scientists (even outside computer science and AI). Consequently, proposing an alternative to YOLO, based mainly on cost optimization, enables readers to get a high-performance alternative (mAP) for less computing resources than the new YOLO (v7,v8,v9).*

Guidelines:

- The answer NA means that there is no societal impact of the work performed.
- If the authors answer NA or No, they should explain why their work has no societal impact or why the paper does not address societal impact.
- Examples of negative societal impacts include potential malicious or unintended uses (e.g., disinformation, generating fake profiles, surveillance), fairness considerations (e.g., deployment of technologies that could make decisions that unfairly impact specific groups), privacy considerations, and security considerations.
- The conference expects that many papers will be foundational research and not tied to particular applications, let alone deployments. However, if there is a direct path to any negative applications, the authors should point it out. For example, it is legitimate to point out that an improvement in the quality of generative models could be used to generate deepfakes for disinformation. On the other hand, it is not needed to point out that a generic algorithm for optimizing neural networks could enable people to train models that generate Deepfakes faster.
- The authors should consider possible harms that could arise when the technology is being used as intended and functioning correctly, harms that could arise when the technology is being used as intended but gives incorrect results, and harms following from (intentional or unintentional) misuse of the technology.
- If there are negative societal impacts, the authors could also discuss possible mitigation strategies (e.g., gated release of models, providing defenses in addition to attacks, mechanisms for monitoring misuse, mechanisms to monitor how a system learns from feedback over time, improving the efficiency and accessibility of ML).

11. **Safeguards**

Question: Does the paper describe safeguards that have been put in place for responsible release of data or models that have a high risk for misuse (e.g., pretrained language models, image generators, or scraped datasets)?

Answer: [NA]

Justification: *Our work contributes to object detection within a very carefully designed dataset: MSCOCO. The paper does not pose such risks.*

Guidelines:

- The answer NA means that the paper poses no such risks.
- Released models that have a high risk for misuse or dual-use should be released with necessary safeguards to allow for controlled use of the model, for example by requiring that users adhere to usage guidelines or restrictions to access the model or implementing safety filters.

- Datasets that have been scraped from the Internet could pose safety risks. The authors should describe how they avoided releasing unsafe images.
- We recognize that providing effective safeguards is challenging, and many papers do not require this, but we encourage authors to take this into account and make a best faith effort.

12. Licenses for existing assets

Question: Are the creators or original owners of assets (e.g., code, data, models), used in the paper, properly credited and are the license and terms of use explicitly mentioned and properly respected?

Answer: [Yes]

Justification: *We have appropriately cited all assets (datasets and code) used in our research. Our work builds upon the open-source AGPL-3.0 licensed YOLOv8 code from Ultralytics. Throughout the paper, we emphasize that we are using code from Ultralytics, highlighting that it is easily reproducible due to the availability of this library.*

Guidelines:

- The answer NA means that the paper does not use existing assets.
- The authors should cite the original paper that produced the code package or dataset.
- The authors should state which version of the asset is used and, if possible, include a URL.
- The name of the license (e.g., CC-BY 4.0) should be included for each asset.
- For scraped data from a particular source (e.g., website), the copyright and terms of service of that source should be provided.
- If assets are released, the license, copyright information, and terms of use in the package should be provided. For popular datasets, `paperswithcode.com/datasets` has curated licenses for some datasets. Their licensing guide can help determine the license of a dataset.
- For existing datasets that are re-packaged, both the original license and the license of the derived asset (if it has changed) should be provided.
- If this information is not available online, the authors are encouraged to reach out to the asset's creators.

13. New Assets

Question: Are new assets introduced in the paper well documented and is the documentation provided alongside the assets?

Answer: [Yes]

Justification: *We have provided the code necessary to build our neural network using the YOLOv8 or YOLOv9 API, along with a comprehensive overview of the architecture schema.*

Guidelines:

- The answer NA means that the paper does not release new assets.
- Researchers should communicate the details of the dataset/code/model as part of their submissions via structured templates. This includes details about training, license, limitations, etc.
- The paper should discuss whether and how consent was obtained from people whose asset is used.
- At submission time, remember to anonymize your assets (if applicable). You can either create an anonymized URL or include an anonymized zip file.

14. Crowdsourcing and Research with Human Subjects

Question: For crowdsourcing experiments and research with human subjects, does the paper include the full text of instructions given to participants and screenshots, if applicable, as well as details about compensation (if any)?

Answer: [NA]

Justification: *The paper does not involve crowdsourcing or research with human subjects.*

Guidelines:

- The answer NA means that the paper does not involve crowdsourcing nor research with human subjects.
- Including this information in the supplemental material is fine, but if the main contribution of the paper involves human subjects, then as much detail as possible should be included in the main paper.
- According to the NeurIPS Code of Ethics, workers involved in data collection, curation, or other labor should be paid at least the minimum wage in the country of the data collector.

15. Institutional Review Board (IRB) Approvals or Equivalent for Research with Human Subjects

Question: Does the paper describe potential risks incurred by study participants, whether such risks were disclosed to the subjects, and whether Institutional Review Board (IRB) approvals (or an equivalent approval/review based on the requirements of your country or institution) were obtained?

Answer: [NA]

Justification: *The paper does not involve crowdsourcing or research with human subjects.*

Guidelines:

- The answer NA means that the paper does not involve crowdsourcing nor research with human subjects.
- Depending on the country in which research is conducted, IRB approval (or equivalent) may be required for any human subjects research. If you obtained IRB approval, you should clearly state this in the paper.
- We recognize that the procedures for this may vary significantly between institutions and locations, and we expect authors to adhere to the NeurIPS Code of Ethics and the guidelines for their institution.
- For initial submissions, do not include any information that would break anonymity (if applicable), such as the institution conducting the review.